J. Plasma Physics (1998), *vol.* 59, *part* 3, *pp.* 505–536. Printed in the United Kingdom
© 1998 Cambridge University Press

Asymptotically matched sheath and presheath in a dense plasma

LINDSEY D. THORNHILL and PRATEEN V. DESAI
George Woodruff School of Mechanical Engineering, Georgia Institute of Technology, Atlanta, Georgia 30332, USA

(Received 8 June 1997 and in revised form 27 October 1997)

Asymptotically matched solutions for electron and ion density, electron and ion velocity, and electric potential are obtained in the boundary region of a dense low-temperature plasma adjacent to perfectly absorbing walls – walls that absorb, without reflection, incident electrons and ions. Leading-order composite solutions, valid throughout the boundary region, are constructed from solutions in three subdomains distinguished by different physical length scales: the geometric length, the ion mean free path and the Debye length. The composite solutions are used to assess the impact of electron–ion recombination in the ionization nonequilibrium region on sheath and presheath profiles, and on quantities evaluated at the wall. While, at leading order, the velocity profiles throughout the boundary region are not influenced by recombination, the density and potential profiles are significantly altered when recombination is included. These results show that the region of rapid change in these profiles lies closer to the wall when recombination is explicitly included in the model. The influence of recombination on the presheath potential, and consequently the wall potential, is found to scale as the natural logarithm of the recombination length. The broadening of the density profile results in a larger flux of ions accelerating through the sheath and impacting on the wall. The influence of recombination on the ion power flux to the wall is found to scale with the inverse recombination length. This scaling influences the prediction of surface erosion rates in technological applications that utilize these plasmas.

1. Introduction

The physics governing the formation of the sheath and presheath at the interface between a plasma and a wall have been studied for some 70 years and are still not fully understood. Among the earliest theoretical investigations into the plasma boundary region were those of Tonks and Langmuir (1929). The basic features of the plasma–sheath transition were revealed in this well-known analysis of a low-pressure plasma column. Tonks and Langmuir identified a field singularity which they described as a 'turning point' in the potential. This singularity was identified using series approximations, in the long-mean-free-path limit, which, for planar geometry, occurred at a potential energy 0.85 times the mean electron energy when ion generation was assumed proportional to electron density. The solution for the plasma potential in the short-mean-free-path limit was found to be singular at the wall. In the Tonks and Langmuir work, the essence of a requirement for the existence of a critical ion velocity at the entrance to the sheath was used in implicit

https://doi.org/10.1017/S0022377898006497 Published online by Cambridge University Press

form, the explicit formulation and interpretation of this requirement being due to Bohm (1949).

The early analyses of the plasma–sheath transition were, for the most part, limited to collisionless plasmas. For collisional plasmas, the approach typically used was to apply linear diffusion theory up to the point where Bohm's criterion was satisfied and then switch to a collisionless sheath model. This approach resulted in an artificial cut-off in the diffusion theory. Persson (1962) pointed out the important role of the nonlinear ion-inertia term in the plasma–sheath transition for collisional plasmas. Persson showed that when ion inertia is considered in the plasma equations, the solutions for both the ion velocity and the plasma density possess singular derivatives at a critical value of ion velocity. This critical velocity was found to be the ambipolar sound speed, provided the wall was assumed to be perfectly absorbing. A perfectly absorbing wall is assumed to absorb incident electrons and ions without any reflection. The ambipolar sound speed corresponds to Bohm's criterion written for a two-temperature plasma, which, Persson concluded, makes Bohm's criterion an integral part of the inertia-controlled diffusion theory.

Self and Ewald (1966) presented a steady-state theory of the quasineutral discharge column, applicable to intermediate pressures, that approximates both the free-fall theory in the low-pressure limit and the Schottky ambipolar-diffusion theory in the high-pressure limit. The ionization source term was taken to be proportional to the electron density. Self and Ewald solved the ambipolar-diffusion equations, retaining the ion-inertia term, for both planar and cylindrical geometries. Analytical solutions were obtained for the planar case and approximate numerical solutions for the cylindrical geometry. As in Persson's analysis, the governing equations clearly exhibit a field singularity when the ion velocity equals the isothermal ion sound speed, indicating the transition to a space-charge-dominated sheath.

Riemann (1991) presented an excellent review of the developments surrounding the analysis of Bohm's criterion, and sheath formation, since it was originally discovered. Riemann used a simple, cold-ion fluid model to illustrate the basic features of the plasma–sheath transition and their relation to Bohm's criterion. He also presented a rigorous kinetic analysis of the vicinity of the sheath edge and showed that the generalized Bohm criterion is, with few special exceptions, marginally fulfilled and related to a field singularity at the sheath edge.

While much of the historical work to date aimed at analysing the plasma sheath and presheath has contributed to the current understanding of plasma boundary layers, much of it is restricted to the analysis of collisionless and weakly collisional plasmas. In cases where a significant degree of collisionality has been allowed, attention has usually been restricted to the presheath region. One notable exception is a work by Friedman (1967). The attention centered around collisionless to weakly collisional plasmas has largely been driven by the interest in low-pressure laboratory arcs, nuclear fusion and low-pressure materials-processing applications.

The goal in this work is to develop solutions for the relevant plasma variables in the boundary region of collisional, near-thermal plasmas. Given this goal, it becomes necessary to explicitly account for the ionization nonequilibrium that can exist in plasmas of this type. This nonequilibrium has been neglected in most previous analyses in favour of a linear electron and ion source term. One exception is the work of Self and Eskin (1983), which was limited to the diffusion-dominated presheath region. The solutions developed here relax the diffusion-dominated assumption of

https://doi.org/10.1017/S0022377898006497 Published online by Cambridge University Press

Self and Eskin and account for the significant variation in properties that occurs throughout the various subdomains that make up the boundary region.

In Sec. 2, a mathematical model describing a collisional, near-thermal plasma is described. In Sec. 3, matched asymptotic analyses are used to develop solutions valid throughout the boundary region. The significance of these solutions are discussed in Sec. 4, followed by closing remarks in Sec. 5.

2. Model development

In this work, interest is restricted to the case of a weakly ionized plasma between planar, parallel, insulating walls separated by a distance $2L$. This system is taken to be one-dimensional, with the origin at the plane of symmetry between the two walls. The plasma is assumed to be isothermal and to consist of electrons and singly charged positive ions in a background of neutral atoms. In this model secondary emission of electrons from the wall has been assumed negligible. Such emission, if it existed, would tend to lower the electric potential near the wall. The plasma is assumed to be free of magnetic fields and to be at, or near, thermodynamic equilibrium. The fluid equations governing the behaviour of such a plasma are the ion and electron continuity equations, the ion and electron momentum equations and Poisson's equation for the electric potential. Given the assumptions made here, these equations may be written respectively as

$$\frac{d}{dx}(n_i v_i) = S_i, \tag{2.1}$$

$$\frac{d}{dx}(n_e v_e) = S_e, \tag{2.2}$$

$$\frac{d}{dx}(m_i n_i v_i^2) + k_b T_i \frac{dn_i}{dx} + e n_i \frac{dV}{dx} + m_i \nu_i n_i v_i = 0, \tag{2.3}$$

$$\frac{d}{dx}(m_e n_e v_e^2) + k_b T_e \frac{dn_e}{dx} - e n_e \frac{dV}{dx} + m_e \nu_e n_e v_e = 0, \tag{2.4}$$

$$\epsilon_0 \frac{d^2 V}{dx^2} + e\,(n_i - n_e) = 0. \tag{2.5}$$

In these equations the subscripts i and e refer to singly charged ions and electrons respectively. Here n is the number density, v is the velocity, T is the temperature, m is the mass and ν is the collision frequency for momentum loss to the neutral gas, for each species. Also, V is the electric potential, k_b is Boltzmann's constant, e is the fundamental charge and ϵ_0 is the free-space permittivity. The relative speeds used to define the collision frequencies in these equations are taken to be the mean thermal speeds for each species. The cross-section for electron–neutral collisions is taken to be the Bohr value for the atomic cross-section. The cross-section for ion–neutral collisions is taken to be twice this value.

The quantities S_i and S_e represent net ion and electron sources respectively. Ion–electron pairs are assumed to be created by the process of electron-impact ionization from the ground state. The rate for this process is $\alpha n_n n_e$, where α is the ionization rate constant and n_n is the neutral number density. In addition to absorption at the wall, electrons and ions are assumed to be lost through the process of three-body recombination into the ground state, with an electron serving as the third body. The rate for this process is $\beta n_i n_e^2$, where β is the recombination rate

https://doi.org/10.1017/S0022377898006497 Published online by Cambridge University Press

coefficient. By assuming no external sources of electrons and ions, the source terms may be expressed as

$$S_i = S_e = \alpha n_n n_e - \beta n_i n_e^2. \tag{2.6}$$

α and β are related through the principle of detailed balance by

$$\frac{\alpha}{\beta} = \frac{n_{\rm eq}^2}{n_n}, \tag{2.7}$$

where $n_{\rm eq}$ is the ion and electron density at ionization equilibrium. Expressions for α and β are derived by Zel'dovich and Raizer (1966) as

$$\alpha = \sigma_e v_{e,\rm th} \left(\frac{I}{k_b T_e} + 2 \right) e^{-I/k_b T_e}, \tag{2.8}$$

$$\beta = \frac{g_n}{g_i} \left(\frac{I}{k_b T_e} + 2 \right) \frac{h^3 \sigma_e}{2\pi^2 m_e^2 k_b T_e}. \tag{2.9}$$

Here σ_e is an average value of the cross-section for electron impact ionization, $v_{e,\rm th}$ is the electron thermal speed, I is the first ionization potential, g_n is the degeneracy for the ground-state neutral, g_i is the degeneracy for the ground-state ion and h is Planck's constant.

At the plane of symmetry, $x = 0$, the boundary conditions are given by

$$n_e = n_c, \quad \frac{dn_e}{dx} = 0, \quad v_i = v_e = 0, \quad V = 0, \tag{2.10}$$

where n_c is the electron density at the centreline, assumed to be maintained by some transverse process such as current conduction. Since the electrons remain essentially Maxwellian near the wall, owing to repulsion by the field, the requirement that the wall collect no net current may be expressed by equating the electron random flux and the ion directed flux. This renders the boundary condition at the wall, $x = L$, as

$$n_i v_i = n_e \left(\frac{k_b T_e}{2\pi m_e} \right)^{1/2}, \tag{2.11}$$

which is the same condition employed by Franklin and Ockendon (1970).

The governing equations are normalized by introducing dimensionless variables defined by

$$\eta_{e,i} = \frac{n_{e,i}}{n_c}, \qquad u_{e,i} = \frac{v_{e,i}}{(k_b T_e/m_i)^{1/2}}, \qquad \phi = \frac{V}{k_b T_e/e}, \qquad \xi = \frac{x}{L}. \tag{2.12}$$

Upon substitution of these dimensionless variables, the system of governing equations becomes

$$\frac{d}{d\xi}(\eta_i u_i) = 2\delta_i \frac{\delta_n^2}{\delta_r^2} \frac{1 + \delta_T}{\delta_T^{1/2} + \frac{1}{2}\delta_m^{1/2}} \eta_e \left(\frac{1}{\delta_n^2} - \eta_i \eta_e \right), \tag{2.13}$$

$$\frac{d}{d\xi}(\eta_e u_e) = 2\delta_i \frac{\delta_n^2}{\delta_r^2} \frac{1 + \delta_T}{\delta_T^{1/2} + \frac{1}{2}\delta_m^{1/2}} \eta_e \left(\frac{1}{\delta_n^2} - \eta_i \eta_e \right), \tag{2.14}$$

$$\frac{d}{d\xi}(\eta_i u_i^2) + \delta_T \frac{d\eta_i}{d\xi} + \eta_i \frac{d\phi}{d\xi} + \frac{\delta_T^{1/2}}{\delta_i} \eta_i u_i = 0, \tag{2.15}$$

https://doi.org/10.1017/S0022377898006497 Published online by Cambridge University Press

$$\delta_m \frac{d}{d\xi}(\eta_e u_e^2) + \frac{d\eta_e}{d\xi} - \eta_e \frac{d\phi}{d\xi} + \frac{1}{2}\frac{\delta_m^{1/2}}{\delta_i}\eta_e u_e = 0, \tag{2.16}$$

$$\frac{\delta_d^2}{\delta_n}\frac{d^2\phi}{d\xi^2} + (\eta_i - \eta_e) = 0, \tag{2.17}$$

subject to the conditions

$$\eta_e = 1, \quad \frac{d\eta_e}{d\xi} = 0, \quad u_i = u_e = 0, \quad \phi = 0 \quad \text{at} \quad \xi = 0, \tag{2.18}$$

and

$$[\eta_i u_i]_{\xi=1} = \left(\frac{1}{2\pi\delta_m}\right)^{1/2} [\eta_e]_{\xi=1} \ . \tag{2.19}$$

Here $\delta_n = n_c/n_{eq}$, $\delta_m = m_e/m_i$ and $\delta_T = T_i/T_e$. This system also contains ratios of length scales given by

$$\delta_r = \frac{l_r}{L}, \qquad \delta_i = \left(\frac{\pi}{8}\right)^{1/2}\frac{l_i}{L}, \qquad \delta_d = \frac{l_d}{L}, \tag{2.20}$$

where l_r is the recombination length, l_i is the ion mean free path and l_d is the Debye length.

There are several parameters in these equations that are potentially quite small. For the conditions of interest in this study, the parameter δ_n, which represents the ratio of the centreline density to the equilibrium density, is less than, but of order, one. Also, as noted earlier, attention is restricted here to plasmas that are at or near thermodynamic equilibrium, i.e. δ_T may be less than, but of order, one. The largest value δ_m can have is the value corresponding to a hydrogen plasma, namely 5×10^{-4}. The remaining parameters in the governing equations, δ_r, δ_i and δ_d, represent ratios of physical length scales to the geometric length. These parameters are typically small, with their relative magnitudes generally given by $1 \gg \delta_r \gg \delta_i \gg \delta_d$.

In order to facilitate interpretation of the roles that these small parameters play in the governing equations, the equations are rearranged. The appearance of the small parameter δ_i in the denominator of the collision terms in the momentum equations can be eliminated by rescaling the electron and ion velocities. This rescaling is accomplished by letting $u_e = \delta_i u_{es}$ and $u_i = \delta_i u_{is}$, where the subscript s indicates the rescaled, normalized variables, and effectively redefines the reference velocity to be the velocity associated with mobility-limited flow. Upon applying this rescaling, the governing equations and boundary conditions become

$$\frac{d}{d\xi}(\eta_i u_{is}) = 2\frac{\delta_n^2}{\delta_r^2}\frac{1+\delta_T}{\delta_T^{1/2} + \frac{1}{2}\delta_m^{1/2}}\eta_e\left(\frac{1}{\delta_n^2} - \eta_i\eta_e\right) \ , \tag{2.21}$$

$$\frac{d}{d\xi}(\eta_e u_{es}) = 2\frac{\delta_n^2}{\delta_r^2}\frac{1+\delta_T}{\delta_T^{1/2} + \frac{1}{2}\delta_m^{1/2}}\eta_e\left(\frac{1}{\delta_n^2} - \eta_i\eta_e\right) \ , \tag{2.22}$$

$$\delta_i^2\frac{d}{d\xi}(\eta_i u_{is}^2) + \delta_T\frac{d\eta_i}{d\xi} + \eta_i\frac{d\phi}{d\xi} + \delta_T^{1/2}\eta_i u_{is} = 0, \tag{2.23}$$

$$\delta_m\delta_i^2\frac{d}{d\xi}(\eta_e u_{es}^2) + \frac{d\eta_e}{d\xi} - \eta_e\frac{d\phi}{d\xi} + \frac{1}{2}\delta_m^{1/2}\eta_e u_{es} = 0, \tag{2.24}$$

https://doi.org/10.1017/S0022377898006497 Published online by Cambridge University Press

$$\frac{\delta_d^2}{\delta_n}\frac{d^2\phi}{d\xi^2} + (\eta_i - \eta_e) = 0\ , \tag{2.25}$$

subject to

$$\eta_e = 1, \quad \frac{d\eta_e}{d\xi} = 0, \quad u_{is} = u_{es} = 0, \quad \phi = 0 \quad \text{at } \xi = 0, \tag{2.26}$$

and

$$[\eta_i u_{is}]_{\xi=1} = \frac{1}{\delta_i}\left(\frac{1}{2\pi\delta_m}\right)^{1/2}[\eta_e]_{\xi=1}\ . \tag{2.27}$$

At present, an exact solution to this system of equations and boundary conditions is not apparent. Furthermore, obtaining approximate solutions by numerical techniques, besides their inherent limitations, is complicated by the disparity in physical length scales that appear in the equations. For these reasons, approximate, analytical solutions to the governing equations are sought.

3. Asymptotic analysis

The system of equations given by (2.21)–(2.25) can be arranged such that each of the length-scale ratios multiplies the highest-order derivative of at least one of the dependent variables, indicating the presence of at least one, and possibly several, boundary layers – the so-called singular perturbation system. Therefore the approach to obtaining approximate analytical solutions is to employ the method of matched asymptotic analysis.

3.1. Solutions on the geometric length scale

The analysis of the governing equations and boundary conditions begins by expressing each of the dependent variables in the system as an asymptotic series in the parameter δ_d, since δ_d is the smallest parameter in the system. This is accomplished by setting $\eta_i = \eta_{i0} + f_1(\delta_d)\,\eta_{i1} + \ldots$, where $\{1, f_1(\delta_d), f_2(\delta_d), \ldots\}$ is an asymptotic sequence of functions, for each dependent variable in the system. The system of equations and boundary conditions that are of leading order with respect to the parameter δ_d are obtained by taking the limit $\delta_d \to 0$.

One consequence of evaluating this limit is that $\eta_{i0} = \eta_{e0}$ everywhere. The continuity equations in the resulting system can be integrated, and boundary conditions at $\xi = 0$ applied, to show that $u_{is0} = u_{es0}$ everywhere. Therefore, by making use of these simplifications, the system that is of leading order with respect to δ_d on the geometric scale is given by

$$\frac{d}{d\xi}(\eta_{i0}u_{is0}) = 2\frac{\delta_n^2}{\delta_r^2}\frac{1+\delta_T}{\delta_T^{1/2} + \frac{1}{2}\delta_m^{1/2}}\eta_{i0}\left(\frac{1}{\delta_n^2} - \eta_{i0}^2\right), \tag{3.1}$$

$$\delta_i^2\frac{d}{d\xi}(\eta_{i0}u_{is0}^2) + \delta_T\frac{d\eta_{i0}}{d\xi} + \eta_{i0}\frac{d\phi_0}{d\xi} + \delta_T^{1/2}\eta_{i0}u_{is0} = 0, \tag{3.2}$$

$$\delta_i^2\delta_m\frac{d}{d\xi}(\eta_{i0}u_{is0}^2) + \frac{d\eta_{i0}}{d\xi} - \eta_{i0}\frac{d\phi_0}{d\xi} + \frac{1}{2}\delta_m^{1/2}\eta_{i0}u_{is0} = 0, \tag{3.3}$$

subject to the conditions

$$\eta_{i0} = 1, \quad \frac{d\eta_{i0}}{d\xi} = 0, \quad \phi_0 = 0 \quad \text{at } \xi = 0, \tag{3.4}$$

https://doi.org/10.1017/S0022377898006497 Published online by Cambridge University Press

and

$$[u_{is0}]_{\xi=1} = \frac{1}{\delta_i}\left(\frac{1}{2\pi\delta_m}\right)^{1/2}. \tag{3.5}$$

This system of equations, which is of leading order with respect to δ_d, is still singular with respect to the parameter δ_i. Therefore the dependent variables are once again expanded by expressing each as an asymptotic series in δ_i, e.g. $\eta_{i0} = \eta_{i00} + g_1(\delta_i)\,\eta_{i01} + \ldots$. From this expansion, the system of equations that are of leading order with respect to both δ_d and δ_i is determined to be

$$\frac{d}{d\xi}(\eta_{i00}u_{is00}) = 2\frac{\delta_n^2}{\delta_r^2}\frac{1+\delta_T}{\delta_T^{1/2}+\frac{1}{2}\delta_m^{1/2}}\eta_{i00}\left(\frac{1}{\delta_n^2}-\eta_{i00}^2\right), \tag{3.6}$$

$$\delta_T\frac{d\eta_{i00}}{d\xi} + \eta_{i00}\frac{d\phi_{00}}{d\xi} + \delta_T^{1/2}\eta_{i00}u_{is00} = 0, \tag{3.7}$$

$$\frac{d\eta_{i00}}{d\xi} - \eta_{i00}\frac{d\phi_{00}}{d\xi} + \frac{1}{2}\delta_m^{1/2}\eta_{i00}u_{is00} = 0, \tag{3.8}$$

subject to the conditions

$$\eta_{i00} = 1, \quad \frac{d\eta_{i00}}{d\xi} = 0, \quad \phi_{00} = 0 \quad \text{at } \xi = 0, \tag{3.9}$$

and

$$[u_{is00}]_{\xi\to 1} \to \infty\,. \tag{3.10}$$

Here the wall boundary condition is effectively lost owing to the reduction in the order of the system of equations.

The solutions to this leading-order system on the geometric length scale can be expressed in terms of Jacobi elliptic functions as

$$\eta_{i00} = \eta_{e00} = \mathrm{sn}(u,k), \tag{3.11}$$

$$u_{i00} = u_{e00} = \delta_i\frac{\delta_n}{\delta_r k}\frac{1+\delta_T}{\delta_T^{1/2}+\frac{1}{2}\delta_m^{1/2}}\frac{\mathrm{cn}(u,k)\,\mathrm{dn}(u,k)}{\mathrm{sn}(u,k)}, \tag{3.12}$$

$$\phi_{00} = \frac{\delta_T^{1/2}-\frac{1}{2}\delta_m^{1/2}\delta_T}{\delta_T^{1/2}+\frac{1}{2}\delta_m^{1/2}}\ln[\mathrm{sn}(u,k)]\,. \tag{3.13}$$

Here $k = [\delta_n^2/(2-\delta_n^2)]^{1/2}$ is the modulus of the elliptic functions and

$$u = K(k) - \frac{\delta_n}{k\delta_r}\xi, \tag{3.14}$$

where $K(k)$ is the complete elliptic integral of the first kind.

There is a physical constraint on the solutions just obtained that should be noted. The density is expected to vary, monotonically, from 1 at the symmetry boundary to some value at the wall, η_w, where $0 \leqslant \eta_w < 1$. Since the elliptic functions are doubly periodic, this physical requirement imposes the condition

$$\frac{\delta_n}{k\delta_r} \leqslant K(k) \tag{3.15}$$

on the solution for the density in order to prevent the solution from passing through zero before the wall is reached. Since k is a function of δ_n only, this condition implies that δ_n and δ_r are not independent parameters. Additional information about the

https://doi.org/10.1017/S0022377898006497 Published online by Cambridge University Press

relationship between these two parameters will be gleaned from the asymptotic matching of solutions.

Of course, this solution cannot satisfy the wall boundary condition, since the velocity tends to infinity as the wall is approached. In order to resolve this difficulty, terms that were neglected on the geometric length scale must be accounted in at least one boundary region. Consideration is first given to the mean-free-path length scale.

3.2. Solutions on the mean-free-path scale

The independent and dependent variables in (3.1)–(3.5) are rescaled by letting

$$\zeta = \frac{\xi - 1}{\delta_i^{\nu}}, \qquad \eta_{i0} = \delta_i^{\lambda_1}\overline{\eta}_{i0}, \qquad u_{is0} = \delta_i^{\lambda_2}\overline{u}_{is0}, \qquad \phi_0 = \delta_i^{\lambda_3}\overline{\phi}_0. \tag{3.16}$$

In order for these scales to be appropriate it is anticipated that $\nu > 0$, $\lambda_1 \geqslant 0$, $\lambda_2 \leqslant 0$ and $\lambda_3 \geqslant 0$. The leading-order balance in the electron momentum equation (3.3) should still be between the pressure gradient and the field term. In the ion momentum equation (3.2), the inertia term, which was neglected on the geometric scale, should be retained, which, at leading order, should be balanced by the field term. Upon requiring these two balances to be satisfied, it is determined that $\lambda_2 = -1$ and $\lambda_3 = 0$. Here it is noted that since $u_{is0} = \delta_i^{-1}\overline{u}_{is0}$, the velocity rescaling imposed in the previous section is effectively removed; therefore the s subscript is dropped.

Upon applying the rescaling determined thus far the governing equations become

$$\frac{d}{d\zeta}(\overline{\eta}_{i0}\overline{u}_{i0}) = \delta_i^{1+\nu} 2\frac{\delta_n^2}{\delta_r^2}\frac{1+\delta_T}{\delta_T^{1/2} + \frac{1}{2}\delta_m^{1/2}}\overline{\eta}_{i0}\left(\frac{1}{\delta_n^2} - \delta_i^{2\lambda_1}\overline{\eta}_{i0}^2\right), \tag{3.17}$$

$$\frac{d}{d\zeta}(\overline{\eta}_{i0}\overline{u}_{i0}^2) + \delta_T\frac{d\overline{\eta}_{i0}}{d\zeta} + \overline{\eta}_{i0}\frac{d\overline{\phi}_0}{d\zeta} + \delta_i^{\nu-1}\delta_T^{1/2}\overline{\eta}_{i0}\overline{u}_{i0} = 0, \tag{3.18}$$

$$\delta_m\frac{d}{d\zeta}(\overline{\eta}_{i0}\overline{u}_{i0}^2) + \frac{d\overline{\eta}_{i0}}{d\zeta} - \overline{\eta}_{i0}\frac{d\overline{\phi}_0}{d\zeta} + \delta_i^{\nu-1}\frac{1}{2}\delta_m^{1/2}\overline{\eta}_{i0}\overline{u}_{i0} = 0, \tag{3.19}$$

with

$$[\overline{u}_{i0}]_{\zeta=0} = \left(\frac{1}{2\pi\delta_m}\right)^{1/2}. \tag{3.20}$$

Only the wall boundary condition is considered here, since the conditions at the symmetry boundary were satisfied on the geometric scale. Several observations can be made about this system of equations. Since $\nu > 0$ and $\lambda_1 \geqslant 0$, neither term on the right-hand side of the continuity equation can be of leading-order. Also, in order to retain the leading-order balances in (3.18) and (3.19), it must hold that $\nu \geqslant 1$.

It has been shown (Thornhill 1996) that the case corresponding to $\nu > 1$ leads to a solution that is physically meaningless. Therefore only the case for $\nu = 1$ is considered here. By taking $\nu = 1$, the system of equations that is of leading order in both δ_d and δ_i on the mean free path scale may be written as

$$\frac{d}{d\zeta}(\overline{\eta}_{i00}\overline{u}_{i00}) = 0, \tag{3.21}$$

$$\frac{d}{d\zeta}(\overline{\eta}_{i00}\overline{u}_{i00}^2) + \delta_T\frac{d\overline{\eta}_{i00}}{d\zeta} + \overline{\eta}_{i00}\frac{d\overline{\phi}_{00}}{d\zeta} + \delta_T^{1/2}\overline{\eta}_{i00}\overline{u}_{i00} = 0, \tag{3.22}$$

https://doi.org/10.1017/S0022377898006497 Published online by Cambridge University Press

$$\delta_m \frac{d}{d\zeta}(\overline{\eta}_{i00}\overline{u}_{i00}^2) + \frac{d\overline{\eta}_{i00}}{d\zeta} - \overline{\eta}_{i00}\frac{d\overline{\phi}_{00}}{d\zeta} + \frac{1}{2}\delta_m^{1/2}\overline{\eta}_{i00}\overline{u}_{i00} = 0, \tag{3.23}$$

subject to

$$[\overline{u}_{i00}]_{\zeta=0} = \left(\frac{1}{2\pi\delta_m}\right)^{1/2}. \tag{3.24}$$

The continuity equation, (3.21), may be integrated immediately, giving

$$\overline{\eta}_{i00}\overline{u}_{i00} = \overline{C}_1, \tag{3.25}$$

where $\overline{C}_1$ is the constant of integration. By using this result, the ion momentum equation can be arranged as

$$(\delta_T - \overline{u}_{i00}^2)\frac{d\overline{\eta}_{i00}}{d\zeta} + \overline{\eta}_{i00}\frac{d\overline{\phi}_{00}}{d\zeta} + \delta_T^{1/2}\overline{C}_1 = 0, \tag{3.26}$$

where it appears that a singularity exists when $\overline{u}_{i00} = \delta_T^{1/2}$, which corresponds to the ion sound speed $(k_bT_i/m_i)^{1/2}$. Since $\delta_T^{1/2} < (2\pi\delta_m)^{-1/2}$, this singularity occurs before the boundary condition is met, and therefore must be removed. Removal of the singularity involves, at least, requiring that

$$\left[\frac{d\overline{\phi}_{00}}{d\zeta}\right]_{\overline{u}_{i00}=\delta_T^{1/2}} = -\delta_T. \tag{3.27}$$

However, this condition can be shown to be satisfied identically, and therefore the singularity requires no special treatment.

Similarly, the electron momentum equation, (3.23), may be arranged as

$$(1 - \delta_m\overline{u}_{i00}^2)\frac{d\overline{\eta}_{i00}}{d\zeta} - \overline{\eta}_{i00}\frac{d\overline{\phi}_{00}}{d\zeta} + \frac{1}{2}\delta_m^{1/2}\overline{C}_1 = 0, \tag{3.28}$$

which has a singularity at $\overline{u}_{i00} = \delta_m^{-1/2}$, which corresponds to the electron sound speed, $(k_bT_e/m_e)^{1/2}$. However, since $\delta_m^{-1/2} > (2\pi\delta_m)^{-1/2}$, this singularity lies outside the domain of interest.

The potential gradient is eliminated by adding the two momentum equations, and after rearranging, this gives

$$\frac{d\overline{u}_{i00}}{d\zeta} = \frac{\dfrac{\delta_T^{1/2} + \frac{1}{2}\delta_m^{1/2}}{1+\delta_m}\overline{u}_{i00}^2}{\dfrac{1+\delta_T}{1+\delta_m} - \overline{u}_{i00}^2}. \tag{3.29}$$

The singularity apparent in this equation occurs before the wall boundary condition is satisfied, since $[(1+\delta_T)/(1+\delta_m)]^{1/2} < (2\pi\delta_m)^{-1/2}$. Therefore the wall boundary condition cannot be satisfied on the mean free path scale, which indicates the presence of at least one additional layer before the wall is reached.

The velocity at the singularity corresponds to the ambipolar sound speed in the plasma. This equation indicates that the one-dimensional ambipolar fluid represented by the model on the mean free path scale cannot be accelerated beyond its sound speed, yielding

$$\overline{u}_{i00} \leqslant \left(\frac{1+\delta_T}{1+\delta_m}\right)^{1/2}. \tag{3.30}$$

https://doi.org/10.1017/S0022377898006497 Published online by Cambridge University Press

The singularity at the ambipolar sound speed indicates the breakdown in the validity of the quasineutral model, as discussed by Riemann (1991).

Upon integrating (3.29) and rearranging, a solution for $\overline{u}_{i00}$ is obtained as

$$\overline{u}_{i00} = \frac{1}{2}\left(\frac{\delta_T^{1/2} + \frac{1}{2}\delta_m^{1/2}}{1+\delta_m}\zeta + \overline{C}_2\right) \times \left\{-1 \pm \left[1 - \frac{4\dfrac{1+\delta_T}{1+\delta_m}}{\left(\dfrac{\delta_T^{1/2} + \frac{1}{2}\delta_m^{1/2}}{1+\delta_m}\zeta + \overline{C}_2\right)^2}\right]^{1/2}\right\}. \tag{3.31}$$

Finally, by subtracting the electron momentum equation from the product of δ_m and the ion momentum equation, a first-order equation for the potential is obtained. After integrating this equation, by making the transformation $d/d\zeta = (d\overline{u}_{i00}/d\zeta)\, d/d\overline{u}_{i00}$, the solution for the potential is obtained as

$$\overline{\phi}_{00} = -\frac{\delta_T^{1/2} - \frac{1}{2}\delta_m^{1/2}\delta_T}{\delta_T^{1/2} + \frac{1}{2}\delta_m^{1/2}} \ln \overline{u}_{i00} + \frac{1}{2}\frac{\delta_m\delta_T^{1/2} - \frac{1}{2}\delta_m^{1/2}}{\delta_T^{1/2} + \frac{1}{2}\delta_m^{1/2}}\overline{u}_{i00}^2 + \overline{C}_3(\zeta), \tag{3.32}$$

where $\overline{C}_3(\zeta)$ is the function of integration, since the integration was performed with respect to $\overline{u}_{i00}(\zeta)$.

So the solutions to the leading-order equations on the mean-free-path scale are given by (3.25), (3.31) and (3.32). The unknowns $\overline{C}_1$, $\overline{C}_2$ and $\overline{C}_3(\zeta)$, and the sign in (3.31) remain to be determined by the matching process. The scaling exponent for the density, λ_1, also remains undetermined.

Owing to the difference in the velocity scales indicated by the rescaling in (3.16), to leading order in both δ_d and δ_i, the ion velocity on the geometric length scale is 0. The Prandtl matching condition therefore requires that

$$\lim_{\zeta\to-\infty} \overline{u}_{i00} = 0, \tag{3.33}$$

which is satisfied by choosing the positive sign in (3.31). However, upon examination of (3.25), it is evident that the condition given in (3.33) implies that $\overline{\eta}_{i00}$ becomes infinite as $\zeta \to -\infty$ unless either $\overline{C}_1$ is zero or the density scales such that $\lambda_1 > 0$. Setting $\overline{C}_1 = 0$ would result in zero ion flux, so it must hold that $\lambda_1 > 0$.

Since the density scale in the mean-free-path region has been taken to be $\delta_i^{\lambda_1}$, for $\lambda_1 > 0$, the density on this scale, to leading order in δ_i, is 0. In this case, the Prandtl matching condition requires that

$$\lim_{\xi\to 1} \eta_{i00} = 0, \tag{3.34}$$

which is satisfied by requiring equality to hold in (3.15). This equality requires that δ_n and δ_r be related, and therefore they are not independent parameters. In light of (3.15) being satisfied with equality, the argument of the Jacobi elliptic functions, u, in the solutions on the geometric length scale becomes $u = K(k)(1-\xi)$.

On the geometric length scale, the ion flux, written in terms of the scaled velocity,

https://doi.org/10.1017/S0022377898006497 Published online by Cambridge University Press

is given as

$$\eta_{i00}u_{is00} = \frac{\delta_n}{\delta_r k}\frac{1+\delta_T}{\delta_T^{1/2}+\frac{1}{2}\delta_m^{1/2}}\mathrm{cn}[K(1-\xi)]\,\mathrm{dn}[K(1-\xi)]\,. \tag{3.35}$$

This ion flux is written in terms of an intermediate variable y by defining $y = (\xi-1)/\delta_i^{\nu_m}$, for $0 < \nu_m \leqslant 1$, so that the flux on the intermediate scale, $(\eta_{i00}u_{is00})^I$, becomes

$$(\eta_{i00}u_{is00})^I = \frac{\delta_n}{\delta_r k}\frac{1+\delta_T}{\delta_T^{1/2}+\frac{1}{2}\delta_m^{1/2}}\mathrm{cn}(-\delta_i^{\nu_m}Ky)\mathrm{dn}(-\delta_i^{\nu_m}Ky). \tag{3.36}$$

Upon using the limit process to expand this function for small δ_i with y fixed, the result

$$(\eta_{i00}u_{is00})^I = \frac{\delta_n}{\delta_r k}\frac{1+\delta_T}{\delta_T^{1/2}+\frac{1}{2}\delta_m^{1/2}} + O(\delta_i^{\nu_m}) \tag{3.37}$$

is obtained.

On the mean-free-path length scale, the ion flux is given by (3.25), where the scaling $\eta_i = \delta_i^{\lambda_1}\overline{\eta}_i$ holds. Since the ion flux must be conserved, $\eta_{i00}u_{is00}$ and $\overline{\eta}_{i00}\overline{u}_{i00}$ must be of the same order, which requires that $\lambda_1 = 1$. $\overline{C}_1$ is then determined by matching the flux, which gives

$$\overline{C}_1 = \frac{\delta_n}{\delta_r k}\frac{1+\delta_T}{\delta_T^{1/2}+\frac{1}{2}\delta_m^{1/2}}. \tag{3.38}$$

Upon making the definitions

$$A = \frac{\delta_T^{1/2}-\frac{1}{2}\delta_m^{1/2}\delta_T}{\delta_T^{1/2}+\frac{1}{2}\delta_m^{1/2}}, \qquad B = \frac{1}{2}\frac{\frac{1}{2}\delta_m^{1/2}-\delta_m\delta_T^{1/2}}{\delta_T^{1/2}+\frac{1}{2}\delta_m^{1/2}},$$

the solutions for the potential on the geometric and mean-free-path length scales may be written as

$$\phi_{00} = A\ln\eta_{i00}, \tag{3.39}$$

$$\overline{\phi}_{00} = -A\ln\overline{u}_{i00} - B\overline{u}_{i00}^2 + \overline{C}_3(\zeta) \tag{3.40}$$

respectively.

The potential on the geometric scale is expressed in terms of the intermediate variable y as

$$(\phi_{00})^I = A\ln[\mathrm{sn}(-\delta_i^{\nu_m}Ky)]. \tag{3.41}$$

This function can be expressed as an infinite series and factored to give

$$(\phi_{00})^I = A\nu_m\ln\delta_i + A\ln K$$

$$+ A\ln\left(-y + \delta_i^{2\nu_m}\frac{1+k^2}{3!}K^2y^3 - \delta_i^{4\nu_m}\frac{1+14k^2+k^4}{5!}K^4y^5 + \ldots\right). \tag{3.42}$$

Upon defining the quantities

$$a = \frac{\delta_T^{1/2}+\frac{1}{2}\delta_m^{1/2}}{1+\delta_m}, \qquad b = \frac{4\,(1+\delta_T)}{1+\delta_m} \tag{3.43}$$

and expressing the square root as a binomial series, the velocity on the mean-free-

https://doi.org/10.1017/S0022377898006497 Published online by Cambridge University Press

path scale can be written in terms of the intermediate variable as

$$(\overline{u}_{i00})^I = \delta_i^{1-\nu_m}\left[-\frac{b}{4}(ay+\delta_i^{1-\nu_m}\overline{C}_2)^{-1} -\delta_i^{2(1-\nu_m)}\frac{b^2}{16}(ay+\delta_i^{1-\nu_m}\overline{C}_2)^{-3}-\ldots\right]. \tag{3.44}$$

After substituting this equation into (3.40) and factoring the $\ln\overline{u}_{i00}$ term, $\overline{\phi}_{00}$ can be written in terms of the intermediate variable as

$$\begin{aligned}(\overline{\phi}_{00})^I = {} & A\nu_m\ln\delta_i - A\ln\left(\frac{b}{4a}\right)\\ & -A\ln\left[-\left(y+\delta_i^{1-\nu_m}\frac{\overline{C}_2}{a}\right)^{-1}-\delta_i^{2(1-\nu_m)}\frac{b}{4a^2}\left(y+\delta_i^{1-\nu_m}\frac{\overline{C}_2}{a}\right)^{-3}-\ldots\right]\\ & -\delta_i^{2(1-\nu_m)}B\left[-\frac{b}{4}\left(ay+\delta_i^{1-\nu_m}\overline{C}_2\right)^{-1}\right.\\ & \left.-\delta_i^{2(1-\nu_m)}\frac{b^2}{16}(ay+\delta_i^{1-\nu_m}\overline{C}_2)^{-3}-\ldots\right]+\overline{C}_3(y).\end{aligned} \tag{3.45}$$

In the limit $\delta_i \to 0$ with y fixed, the leading-order terms in (3.42) and (3.45) become

$$(\phi_{00})^I \approx A\nu_m\ln\delta_i + A\ln(-y) + A\ln K, \tag{3.46}$$

$$(\overline{\phi}_{00})^I \approx A(\nu_m-1)\ln\delta_i + A\ln(-y) - A\ln\left(\frac{b}{4a}\right)+\overline{C}_3(y). \tag{3.47}$$

By equating these two expressions, the result

$$\overline{C}_3 = \frac{\delta_T^{1/2}-\frac{1}{2}\delta_m^{1/2}\delta_T}{\delta_T^{1/2}+\frac{1}{2}\delta_m^{1/2}}\ln\left[\delta_i\frac{\delta_n}{\delta_r k}\left(\frac{1+\delta_T}{\delta_T^{1/2}+\frac{1}{2}\delta_m^{1/2}}\right)\right] \tag{3.48}$$

is obtained.

After matching, the solutions on the geometric length scale become

$$\eta_{i00} = \eta_{e00} = \mathrm{sn}(u,k), \tag{3.49}$$

$$u_{i00} = u_{e00} = \delta_i\frac{\delta_n}{\delta_r k}\frac{1+\delta_T}{\delta_T^{1/2}+\frac{1}{2}\delta_m^{1/2}}\frac{\mathrm{cn}(u,k)\,\mathrm{dn}(u,k)}{\mathrm{sn}(u,k)}, \tag{3.50}$$

$$\phi_{00} = \frac{\delta_T^{1/2}-\frac{1}{2}\delta_m^{1/2}\delta_T}{\delta_T^{1/2}+\frac{1}{2}\delta_m^{1/2}}\ln[\mathrm{sn}(u,k)], \tag{3.51}$$

with $u = K(k)(1-\xi)$and $\delta_n/\delta_r k = K(k)$. The solutions on the mean-free-path length scale become

$$\overline{\eta}_{i00}\overline{u}_{i00} = \overline{\eta}_{e00}\overline{u}_{e00} = \frac{\delta_n}{\delta_r k}\frac{1+\delta_T}{\delta_T^{1/2}+\frac{1}{2}\delta_m^{1/2}}, \tag{3.52}$$

https://doi.org/10.1017/S0022377898006497 Published online by Cambridge University Press

$$\overline{u}_{i00} = \overline{u}_{e00} = \frac{1}{2}\left(\frac{\delta_T^{1/2} + \frac{1}{2}\delta_m^{1/2}}{1+\delta_m}\zeta + \overline{C}_2\right) \times \left\{-1 + \left[1 - \frac{4\dfrac{1+\delta_T}{1+\delta_m}}{\left(\dfrac{\delta_T^{1/2} + \frac{1}{2}\delta_m^{1/2}}{1+\delta_m}\zeta + \overline{C}_2\right)^2}\right]^{1/2}\right\}, \tag{3.53}$$

$$\overline{\phi}_{00} = \frac{\delta_T^{1/2} - \frac{1}{2}\delta_m^{1/2}\delta_T}{\delta_T^{1/2} + \frac{1}{2}\delta_m^{1/2}} \ln(\delta_i \overline{\eta}_{i00}) - \frac{1}{2}\frac{\frac{1}{2}\delta_m^{1/2} - \delta_m\delta_T^{1/2}}{\delta_T^{1/2} + \frac{1}{2}\delta_m^{1/2}}\overline{u}_{i00}^2. \tag{3.54}$$

In these equations, the constant $\overline{C}_2$ must be determined by matching the mean-free-path solutions to the sheath.

In order to match the solutions on the mean-free-path scale to the solutions in the sheath, which are developed in the following section, the Prandtl matching conditions will be required. These conditions are derived by evaluating the limit $\zeta \to 0^-$ in the solutions above. This evaluation leads to

$$\lim_{\zeta\to 0^-} \overline{\eta}_{i00}\overline{u}_{i00} = \lim_{\zeta\to 0^-} \overline{\eta}_{e00}\overline{u}_{e00} = \frac{\delta_n}{\delta_r k}\frac{1+\delta_T}{\delta_T^{1/2} + \frac{1}{2}\delta_m^{1/2}}, \tag{3.55}$$

$$\lim_{\zeta\to 0^-} \overline{u}_{i00} = \lim_{\zeta\to 0^-} \overline{u}_{e00} = \tfrac{1}{2}\overline{C}_2\left[-1 + \left(1 - \frac{4}{\overline{C}_2^2}\frac{1+\delta_T}{1+\delta_m}\right)^{1/2}\right], \tag{3.56}$$

$$\lim_{\zeta\to 0^-} \overline{\phi}_{00} = \frac{\delta_T^{1/2} - \frac{1}{2}\delta_m^{1/2}\delta_T}{\delta_T^{1/2} + \frac{1}{2}\delta_m^{1/2}} \ln\delta_i + \frac{\delta_T^{1/2} - \frac{1}{2}\delta_m^{1/2}\delta_T}{\delta_T^{1/2} + \frac{1}{2}\delta_m^{1/2}} \ln\left\{\frac{\dfrac{\delta_n}{\delta_r k}\dfrac{1+\delta_T}{\delta_T^{1/2} + \frac{1}{2}\delta_m^{1/2}}}{\frac{1}{2}\overline{C}_2\left[-1 + \left(1 - \frac{4}{\overline{C}_2^2}\dfrac{1+\delta_T}{1+\delta_m}\right)^{1/2}\right]}\right\} - \frac{1}{8}\frac{\frac{1}{2}\delta_m^{1/2} - \delta_m\delta_T^{1/2}}{\delta_T^{1/2} + \frac{1}{2}\delta_m^{1/2}}\overline{C}_2^2\left[-1 + \left(1 - \frac{4}{\overline{C}_2^2}\frac{1+\delta_T}{1+\delta_m}\right)^{1/2}\right]^2. \tag{3.57}$$

3.3. Solutions on the Debye length scale

Now, solutions in the space-charge-dominated sheath, which scales as some function of δ_d, must be resolved. The governing equations and the wall boundary condition, given by (2.13)–(2.17) along with the condition (2.19), are cast on the Debye length scale by letting

$$\theta = \frac{\xi - 1}{\delta_d^{\overline{\nu}}}, \tag{3.58}$$

$$\eta_i = \delta_d^{\overline{\lambda}_1}\widetilde{\eta}_i, \qquad \eta_e = \delta_d^{\overline{\lambda}_2}\widetilde{\eta}_e, \tag{3.59}$$

https://doi.org/10.1017/S0022377898006497 Published online by Cambridge University Press

$$u_i = \delta_d^{\overline{\lambda}_3}\widetilde{u}_i, \qquad u_e = \delta_d^{\overline{\lambda}_4}\widetilde{u}_e, \tag{3.60}$$

$$\phi = \delta_d^{\overline{\lambda}_5}\widetilde{\phi}. \tag{3.61}$$

Based on the anticipated behaviour of the solutions, it is expected that

$$\overline{\nu} > 0, \qquad \overline{\lambda}_1, \overline{\lambda}_2 \geqslant 0, \qquad \overline{\lambda}_3, \overline{\lambda}_4, \overline{\lambda}_5 \leqslant 0$$

in order for the variables to be appropriately scaled. In the sheath, the dominant balance in the electron momentum equation is still expected to be between the pressure gradient and the field term. This balance gives $\overline{\lambda}_5 = 0$. The dominant balance in the ion momentum equation is still expected to be between the inertia term and the field term. This balance gives $\overline{\lambda}_3 = \frac{1}{2}\overline{\lambda}_5 = 0$. Upon balancing the two terms in the wall boundary condition, requiring the boundary condition to be satisfied at leading order, the expression $\overline{\lambda}_2 = \overline{\lambda}_1$ results. Since each ionization or recombination event results in the creation or loss respectively of one electron–ion pair, the continuity source terms should scale identically for both electrons and ions. By requiring this identical scaling, the result $\overline{\lambda}_4 = 0$ is obtained. Upon substitution of these rescaled variables, the governing equations become

$$\frac{d}{d\theta}\left(\widetilde{\eta}_i\widetilde{u}_i\right) = \delta_d^{\overline{\nu}} 2\delta_i \frac{\delta_n^2}{\delta_r^2}\frac{1+\delta_T}{\delta_T^{1/2}+\frac{1}{2}\delta_m^{1/2}}\widetilde{\eta}_e\left(\frac{1}{\delta_n^2} - \delta_d^{2\overline{\lambda}_1}\widetilde{\eta}_i\widetilde{\eta}_e\right), \tag{3.62}$$

$$\frac{d}{d\theta}\left(\widetilde{\eta}_e\widetilde{u}_e\right) = \delta_d^{\overline{\nu}} 2\delta_i \frac{\delta_n^2}{\delta_r^2}\frac{1+\delta_T}{\delta_T^{1/2}+\frac{1}{2}\delta_m^{1/2}}\widetilde{\eta}_e\left(\frac{1}{\delta_n^2} - \delta_d^{2\overline{\lambda}_1}\widetilde{\eta}_i\widetilde{\eta}_e\right), \tag{3.63}$$

$$\frac{d}{d\theta}\left(\widetilde{\eta}_i\widetilde{u}_i^2\right) + \delta_T\frac{d\widetilde{\eta}_i}{d\theta} + \widetilde{\eta}_i\frac{d\widetilde{\phi}}{d\theta} + \delta_d^{\overline{\nu}}\frac{\delta_T^{1/2}}{\delta_i}\widetilde{\eta}_i\widetilde{u}_i = 0, \tag{3.64}$$

$$\delta_m\frac{d}{d\theta}\left(\widetilde{\eta}_e\widetilde{u}_e^2\right) + \frac{d\widetilde{\eta}_e}{d\theta} - \widetilde{\eta}_e\frac{d\widetilde{\phi}}{d\theta} + \delta_d^{\overline{\nu}}\frac{1}{2}\frac{\delta_m^{1/2}}{\delta_i}\widetilde{\eta}_e\widetilde{u}_e = 0, \tag{3.65}$$

$$\delta_d^{2-2\overline{\nu}-\overline{\lambda}_1}\frac{d^2\widetilde{\phi}}{d\theta^2} + \delta_n\left(\widetilde{\eta}_i - \widetilde{\eta}_e\right) = 0, \tag{3.66}$$

with

$$\left[\widetilde{\eta}_i\widetilde{u}_i\right]_{\theta=0} = \left(\frac{1}{2\pi\delta_m}\right)^{1/2}\left[\widetilde{\eta}_e\right]_{\theta=0}\ . \tag{3.67}$$

In these equations, it is clear that for any $\overline{\nu} > 0$ and $\overline{\lambda}_1 \geqslant 0$, the source terms in the continuity equations and the collision terms in the momentum equations cannot be of leading order. However, in general, $2 - 2\overline{\nu} - \overline{\lambda}_1 \geqslant 0$ since the Laplacian must balance the space charge $\widetilde{\eta}_i - \widetilde{\eta}_e$ at some order. The principal physical mechanism that comes into focus in the sheath is this influence of space charge. For this reason, the case $2 - 2\overline{\nu} - \overline{\lambda}_1 = 0$, which requires the Laplacian in Poisson's equation to balance space charge, is considered first. Since it is expected that $\overline{\lambda}_1 \geqslant 0$ and that $\overline{\nu} > 0$, it must hold that $0 < \overline{\nu} \leqslant 1$.

Upon substitution of the rescaled variables, the governing equations in the sheath become

$$\frac{d}{d\theta}\left(\widetilde{\eta}_i\widetilde{u}_i\right) = \delta_d^{\overline{\nu}} 2\delta_i \frac{\delta_n^2}{\delta_r^2}\frac{1+\delta_T}{\delta_T^{1/2}+\frac{1}{2}\delta_m^{1/2}}\widetilde{\eta}_e\left(\frac{1}{\delta_n^2} - \delta_d^{4-4\overline{\nu}}\widetilde{\eta}_i\widetilde{\eta}_e\right), \tag{3.68}$$

https://doi.org/10.1017/S0022377898006497 Published online by Cambridge University Press

$$\frac{d}{d\theta}\,(\widetilde{\eta}_e\widetilde{u}_e) = \delta_d^{\overline{\nu}} 2\delta_i \frac{\delta_n^2}{\delta_r^2}\frac{1+\delta_T}{\delta_T^{1/2}+\frac{1}{2}\delta_m^{1/2}}\widetilde{\eta}_e\left(\frac{1}{\delta_n^2}-\delta_d^{4-4\overline{\nu}}\widetilde{\eta}_i\widetilde{\eta}_e\right), \tag{3.69}$$

$$\frac{d}{d\theta}(\widetilde{\eta}_i\widetilde{u}_i^2)+\delta_T\frac{d\widetilde{\eta}_i}{d\theta}+\widetilde{\eta}_i\frac{d\widetilde{\phi}}{d\theta}+\delta_d^{\overline{\nu}}\frac{\delta_T^{1/2}}{\delta_i}\widetilde{\eta}_i\widetilde{u}_i=0, \tag{3.70}$$

$$\delta_m\frac{d}{d\theta}(\widetilde{\eta}_e\widetilde{u}_e^2)+\frac{d\widetilde{\eta}_e}{d\theta}-\widetilde{\eta}_e\frac{d\widetilde{\phi}}{d\theta}+\delta_d^{\overline{\nu}}\frac{1}{2}\frac{\delta_m^{1/2}}{\delta_i}\widetilde{\eta}_e\widetilde{u}_e=0, \tag{3.71}$$

$$\frac{d^2\widetilde{\phi}}{d\theta^2}+\delta_n\,(\widetilde{\eta}_i-\widetilde{\eta}_e)=0, \tag{3.72}$$

subject to

$$[\widetilde{\eta}_i\widetilde{u}_i]_{\theta=0}=\left(\frac{1}{2\pi\delta_m}\right)^{1/2}[\widetilde{\eta}_e]_{\theta=0}\ . \tag{3.73}$$

In this system, the scale $\overline{\nu}$, and hence $\overline{\lambda}_1\ (=2-2\overline{\nu})$, remain undetermined; however, it is known that $0<\overline{\nu}\leqslant 1$.

The system of equations on the Debye length scale that are of leading order with respect to δ_i and δ_d are derived by expanding the dependent variables as asymptotic series in each of these parameters and evaluating the limits $\delta_i\to 0$ and $\delta_d\to 0$. The result is

$$\frac{d}{d\theta}\,(\widetilde{\eta}_{i00}\widetilde{u}_{i00})=0, \tag{3.74}$$

$$\frac{d}{d\theta}\,(\widetilde{\eta}_{e00}\widetilde{u}_{e00})=0, \tag{3.75}$$

$$\frac{d}{d\theta}(\widetilde{\eta}_{i00}\widetilde{u}_{i00}^2)+\delta_T\frac{d\widetilde{\eta}_{i00}}{d\theta}+\widetilde{\eta}_{i00}\frac{d\widetilde{\phi}_{00}}{d\theta}=0, \tag{3.76}$$

$$\delta_m\frac{d}{d\theta}(\widetilde{\eta}_{e00}\widetilde{u}_{e00}^2)+\frac{d\widetilde{\eta}_{e00}}{d\theta}-\widetilde{\eta}_{e00}\frac{d\widetilde{\phi}_{00}}{d\theta}=0, \tag{3.77}$$

$$\frac{d^2\widetilde{\phi}_{00}}{d\theta^2}+\delta_n\,(\widetilde{\eta}_{i00}-\widetilde{\eta}_{e00})=0, \tag{3.78}$$

with

$$[\widetilde{\eta}_{i00}\widetilde{u}_{i00}]_{\theta=0}=\left(\frac{1}{2\pi\delta_m}\right)^{1/2}[\widetilde{\eta}_{e00}]_{\theta=0}\ . \tag{3.79}$$

The continuity equations are integrated to give

$$\widetilde{\eta}_{i00}\widetilde{u}_{i00}=\widetilde{C}_1,\qquad \widetilde{\eta}_{e00}\widetilde{u}_{e00}=\widetilde{C}_2, \tag{3.80}$$

where $\widetilde{C}_1$ and $\widetilde{C}_2$ are the constants of integration. The momentum equations are added and then integrated to give

$$(\widetilde{u}_{i00}^2-\delta_T\ln\widetilde{u}_{i00}^2)+(\delta_m\widetilde{u}_{e00}^2-\ln(\widetilde{u}_{e00}^2)=\widetilde{C}_3, \tag{3.81}$$

which relates $\widetilde{u}_{i00}$ and $\widetilde{u}_{e00}$.

By differentiating the ion momentum equation, and making several substitutions, the second-order equation

$$\frac{d^2}{d\theta^2}(\widetilde{u}_{i00}^2-\delta_T\ln\widetilde{u}_{i00}^2)=2\delta_n\left(\frac{\widetilde{C}_1}{\widetilde{u}_{i00}}-\frac{\widetilde{C}_2}{\widetilde{u}_{e00}}\right) \tag{3.82}$$

https://doi.org/10.1017/S0022377898006497 Published online by Cambridge University Press

is obtained. Upon defining $\psi = \widetilde{u}_{i00}^2 - \delta_T \ln \widetilde{u}_{i00}^2$, and multiplying (3.82) by the integrating factor $d\psi/d\theta$, the first integral is evaluated as

$$\left(\frac{d\psi}{d\theta}\right)^2 = 4\delta_n \left(\int \frac{\widetilde{C}_1}{\widetilde{u}_{i00}} \frac{d\psi}{d\theta} d\theta - \int \frac{\widetilde{C}_2}{\widetilde{u}_{e00}} \frac{d\psi}{d\theta} d\theta + \widetilde{C}_4 \right). \tag{3.83}$$

After evaluation of these two integrals, (3.83) may be expressed in terms of the electron and ion velocities as

$$\frac{d\widetilde{u}_{i00}}{d\theta} = \pm(2\delta_n)^{1/2} \frac{[\widetilde{C}_1 (\widetilde{u}_{i00} + \delta_T/\widetilde{u}_{i00}) + \widetilde{C}_2 (\delta_m \widetilde{u}_{e00} + 1/\widetilde{u}_{e00}) + \widetilde{C}_4]^{1/2}}{\widetilde{u}_{i00} - \delta_T/\widetilde{u}_{i00}}. \tag{3.84}$$

It is not apparent that an analytical solution to (3.84) is possible; however, by relating $\widetilde{u}_{e00}$ to $\widetilde{u}_{i00}$ through (3.81) and using the wall boundary condition as an initial condition, the integral solution, given by

$$\widetilde{u}_{i00} = \pm(2\delta_n)^{1/2} \int_{-\infty}^{\theta} \frac{[\widetilde{C}_1 (\widetilde{u}_{i00} + \delta_T/\widetilde{u}_{i00}) + \widetilde{C}_2 (\delta_m \widetilde{u}_{e00} + 1/\widetilde{u}_{e00}) + \widetilde{C}_4]^{1/2}}{\widetilde{u}_{i00} - \delta_T/\widetilde{u}_{i00}} d\theta', \tag{3.85}$$

may be evaluated numerically. It will be shown through asymptotic matching that the singularity at $\widetilde{u}_{i00} = \delta_T^{1/2}$, the ion sound speed, in this equation poses no difficulty.

Finally, the solution for $\widetilde{\phi}_{00}$ is obtained by integrating the ion momentum equation to yield

$$\widetilde{\phi}_{00} = -\tfrac{1}{2}(\widetilde{u}_{i00}^2 - \delta_T \ln \widetilde{u}_{i00}^2) + \widetilde{C}_5. \tag{3.86}$$

The constants of integration $\widetilde{C}_1$, $\widetilde{C}_2$, $\widetilde{C}_3$, $\widetilde{C}_4$ and $\widetilde{C}_5$, and the sign in (3.85) must be determined by matching. As $\theta \to -\infty$, both the electron flux and the ion flux must approach the same value, which is also the value given by $\lim_{\zeta \to 0} \left(\overline{\eta}_{i00} \overline{u}_{i00}\right)$. This limit is known, from the solution on the mean-free-path scale, to be $\overline{C}_1$; therefore it must hold that

$$\widetilde{C}_1 = \widetilde{C}_2 = \overline{C}_1 = \frac{\delta_n}{\delta_r k} \frac{1 + \delta_T}{\delta_T^{1/2} + \frac{1}{2}\delta_m^{1/2}}. \tag{3.87}$$

Given this relationship, and the fact that $\overline{u}_{i00}$ and $\widetilde{u}_{i00}$ are of the same scale, it is necessary that $\overline{\eta}_{i00}$ and $\widetilde{\eta}_{i00}$ be scaled identically, i.e. $\delta_d^{\overline{\lambda}_1} = \delta_i$. Consequently, $\overline{\lambda}_1 = \ln \delta_i / \ln \delta_d$, and therefore $\overline{\nu} = 1 - \frac{1}{2} \ln \delta_i / \ln \delta_d$.

Since the electron and ion velocities are equal on the mean-free-path scale, these velocities on the Debye scale must approach the same value as $\theta \to -\infty$. Therefore the Prandtl matching condition requires that

$$\begin{aligned} \lim_{\theta \to -\infty} \widetilde{u}_{i00} &= \lim_{\theta \to -\infty} \widetilde{u}_{e00} = \lim_{\zeta \to 0^-} \overline{u}_{i00} \\ &= \frac{1}{2}\overline{C}_2 \left[-1 + \left(1 - 4 \frac{1 + \delta_T}{1 + \delta_m} \overline{C}_2^{-2} \right)^{1/2} \right] = \widetilde{u}_\infty. \end{aligned} \tag{3.88}$$

However, $\overline{C}_2$, and consequently the velocity at the sheath edge, remain undetermined.

It can be shown (Thornhill 1996) that physically realizable (monotonic) solutions for the sheath potential can be obtained from this system only if $\widetilde{u}_\infty \geqslant [(1 + \delta_T) / (1 + \delta_m)]^{1/2}$, which is the two-temperature form of Bohm's criterion. However, on the mean-free-path scale, the existence of a field singularity leads

https://doi.org/10.1017/S0022377898006497 Published online by Cambridge University Press

to the condition $\overline{u}_{i00}(\zeta \to 0) = \widetilde{u}_\infty \leqslant [(1+\delta_T)/(1+\delta_m)]^{1/2}$. The only way for both of these conditions to be satisfied is for $\widetilde{u}_\infty = [(1+\delta_T)/(1+\delta_m)]^{1/2}$ to hold.

The case corresponding to the condition $2 - 2\overline{\nu} - \overline{\lambda}_1 > 0$ leads to an intermediate region between the mean-free-path scale and the sheath scale. It was demonstrated by Thornhill (1996) that, at leading order, the solution on this scale collapses to a point. This result will need to be reexamined when first-order influences are considered. In a review article on Bohm's criterion and sheath formation Riemann (1991) makes the point that, strictly speaking, Bohm's criterion refers exclusively to the sheath edge in the asymptotic limit $\delta_d \to 0$. Since, in real situations, δ_d may be small, but never exactly zero, the influence of space charge will be felt before Bohm's criterion is satisfied. In fact, in Franklin and Ockendon's (1970) analysis of a collisionless, cold-ion plasma, with ionization proportional to electron density, plasma and sheath solutions were asymptotically matched, at leading order in δ_d, with Bohm's criterion satisfied by the equality. Once first-order influences were considered, a transition layer between the plasma and sheath was required in order to match solutions in the two regions.

Upon concluding that $\overline{u}_{i00}\left(\zeta \to 0^-\right) = \widetilde{u}_{i00}(\theta \to -\infty) = [(1+\delta_T)/(1+\delta_m)]^{1/2}$, the constant $\overline{C}_2$ is determined to be

$$\overline{C}_2 = -2\left(\frac{1+\delta_T}{1+\delta_m}\right)^{1/2}. \tag{3.89}$$

By noting that $[(1+\delta_T)/(1+\delta_m)]^{1/2} > \delta_T^{1/2}$, it is clear that the singularity in (3.84) is outside the domain of validity for the Debye-scale solution. After applying the limits in (3.88), the result

$$\widetilde{C}_3 = (1+\delta_T)\left[1 - \ln\left(\frac{1+\delta_T}{1+\delta_m}\right)\right] \tag{3.90}$$

is obtained. Since the ion velocity asymptotes to a constant as $\theta \to -\infty$, its derivative must approach zero. By applying this limit to (3.84), $\widetilde{C}_4$ is determined to be

$$\widetilde{C}_4 = -2\frac{\delta_n}{\delta_r k}\frac{(1+\delta_T)(1+\delta_m)}{\delta_T^{1/2} + \frac{1}{2}\delta_m^{1/2}}\left(\frac{1+\delta_T}{1+\delta_m}\right)^{1/2}. \tag{3.91}$$

Prandtl's matching condition for the potential is given by

$$\lim_{\theta\to-\infty}\widetilde{\phi}_{00} = \lim_{\zeta\to0^-}\overline{\phi}_{00}. \tag{3.92}$$

After evaluating these limits the expressions

$$\lim_{\zeta\to0^-}\overline{\phi}_{00} = A\ln\delta_i + A\ln\overline{C}_1 - A\ln\widetilde{u}_\infty - B\widetilde{u}_\infty^2, \tag{3.93}$$

$$\lim_{\theta\to-\infty}\widetilde{\phi}_{00} = \delta_T\ln\widetilde{u}_\infty - \tfrac{1}{2}\widetilde{u}_\infty^2 + \widetilde{C}_5 \tag{3.94}$$

are obtained. By equating these two expressions, $\widetilde{C}_5$ is determined as

$$\begin{aligned}\widetilde{C}_5 = {} & \frac{1}{2}\frac{\delta_T^{1/2}(1+\delta_T)}{\delta_T^{1/2} + \frac{1}{2}\delta_m^{1/2}}\left[1 - \ln\left(\frac{1+\delta_T}{1+\delta_m}\right)\right] \\ & + \frac{\delta_T^{1/2} - \frac{1}{2}\delta_m^{1/2}\delta_T}{\delta_T^{1/2} + \frac{1}{2}\delta_m^{1/2}}\ln\left(\delta_i\frac{\delta_n}{\delta_r k}\frac{1+\delta_T}{\delta_T^{1/2} + \frac{1}{2}\delta_m^{1/2}}\right).\end{aligned} \tag{3.95}$$

https://doi.org/10.1017/S0022377898006497 Published online by Cambridge University Press

Finally, by noting that the velocities entering the sheath are positive, the positive sign is chosen in (3.85).

In summary, the solution on the Debye length scale may now be written as

$$\widetilde{\eta}_{i00}\widetilde{u}_{i00} = \frac{\delta_n}{\delta_r k}\frac{1+\delta_T}{\delta_T^{1/2}+\frac{1}{2}\delta_m^{1/2}}, \tag{3.96}$$

$$\widetilde{\eta}_{e00}\widetilde{u}_{e00} = \frac{\delta_n}{\delta_r k}\frac{1+\delta_T}{\delta_T^{1/2}+\frac{1}{2}\delta_m^{1/2}}, \tag{3.97}$$

$$(\widetilde{u}_{i00}^2 - \delta_T \ln \widetilde{u}_{i00}^2) + (\delta_m \widetilde{u}_{e00}^2 - \ln \widetilde{u}_{e00}^2) = (1+\delta_T)\left[1 - \ln\left(\frac{1+\delta_T}{1+\delta_m}\right)\right], \tag{3.98}$$

$$\widetilde{\phi}_{00} = -\tfrac{1}{2}(\widetilde{u}_{i00}^2 - \delta_T \ln \widetilde{u}_{i00}^2) + \frac{1}{2}\frac{\delta_T^{1/2}(1+\delta_T)}{\delta_T^{1/2}+\frac{1}{2}\delta_m^{1/2}}\left[1 - \ln\left(\frac{1+\delta_T}{1+\delta_m}\right)\right] + \frac{\delta_T^{1/2} - \frac{1}{2}\delta_m^{1/2}\delta_T}{\delta_T^{1/2}+\frac{1}{2}\delta_m^{1/2}} \ln\left(\delta_i \frac{\delta_n}{\delta_r k}\frac{1+\delta_T}{\delta_T^{1/2}+\frac{1}{2}\delta_m^{1/2}}\right), \tag{3.99}$$

$$\widetilde{u}_{i00} = \left(2\frac{\delta_n^2}{\delta_r k}\frac{1+\delta_T}{\delta_T^{1/2}+\frac{1}{2}\delta_m^{1/2}}\right)^{1/2} \times \int_{-\infty}^{\theta} \frac{\{(\widetilde{u}_{i00} + \delta_T/\widetilde{u}_{i00}) + (\delta_m \widetilde{u}_{e00} + 1/\widetilde{u}_{e00}) - 2[(1+\delta_m)(1+\delta_T)]^{1/2}\}^{1/2}}{\widetilde{u}_{i00} - \delta_T/\widetilde{u}_{i00}} d\theta', \tag{3.100}$$

where

$$[\widetilde{\eta}_{i00}\widetilde{u}_{i00}]_{\theta=0} = \left(\frac{1}{2\pi\delta_m}\right)^{1/2} [\widetilde{\eta}_{e00}]_{\theta=0} \ . \tag{3.101}$$

From these solutions, the Debye scale expressions for the potential and ion velocity at the wall may be derived. The ion velocity at the wall, $\widetilde{u}_w$, is determined from

$$\widetilde{u}_w^2 - \delta_T \ln \widetilde{u}_w^2 = (1+\delta_T)\left[1 - \ln\left(\frac{1+\delta_T}{1+\delta_m}\right)\right] - \left[\frac{1}{2\pi} - \ln\left(\frac{1}{2\pi\delta_m}\right)\right], \tag{3.102}$$

and the value of the potential at the wall, $\widetilde{\phi}_w$, is given by

$$\widetilde{\phi}_w = -\ln\left[\left(\frac{1}{2\pi\delta_m}\right)^{1/2}\right] + \frac{1}{4\pi} - \frac{\frac{1}{4}\delta_m^{1/2}(1+\delta_T)}{\delta_T^{1/2}+\frac{1}{2}\delta_m^{1/2}}\left[1 - \ln\left(\frac{1+\delta_T}{1+\delta_m}\right)\right] + \frac{\delta_T^{1/2} - \frac{1}{2}\delta_m^{1/2}\delta_T}{\delta_T^{1/2}+\frac{1}{2}\delta_m^{1/2}} \ln\left(\delta_i \frac{\delta_n}{\delta_r k}\frac{1+\delta_T}{\delta_T^{1/2}+\frac{1}{2}\delta_m^{1/2}}\right). \tag{3.103}$$

The potential decrease in the presheath region is given by (3.93) as

$$\overline{\phi}_{ps} = \frac{\delta_T^{1/2} - \frac{1}{2}\delta_m^{1/2}\delta_T}{\delta_T^{1/2}+\frac{1}{2}\delta_m^{1/2}} \ln\left(\delta_i \frac{\delta_n}{\delta_r k}\frac{1+\delta_T}{\delta_T^{1/2}+\frac{1}{2}\delta_m^{1/2}}\right) - \frac{1}{2}\frac{\frac{1}{2}\delta_m^{1/2} - \delta_m\delta_T^{1/2}}{\delta_T^{1/2}+\frac{1}{2}\delta_m^{1/2}}\frac{1+\delta_T}{1+\delta_m}. \tag{3.104}$$

https://doi.org/10.1017/S0022377898006497 Published online by Cambridge University Press

Finally, the potential decrease in the sheath is given as

$$\widetilde{\phi}_s = \widetilde{\phi}_w - \overline{\phi}_{ps} = -\ln\left[\left(\frac{1}{2\pi\delta_m}\right)^{1/2}\right] + \frac{1}{4\pi} - \frac{\frac{1}{4}\delta_m^{1/2}(1+\delta_T)}{\delta_T^{1/2}+\frac{1}{2}\delta_m^{1/2}}\left[1-\ln\left(\frac{1+\delta_T}{1+\delta_m}\right)\right] + \frac{1}{2}\frac{\frac{1}{2}\delta_m^{1/2}-\delta_m\delta_T^{1/2}}{\delta_T^{1/2}+\frac{1}{2}\delta_m^{1/2}}\frac{1+\delta_T}{1+\delta_m}. \quad (3.105)$$

3.4. Composite solutions

While a great deal of information about the solutions to the system of governing equations can be derived from the solutions in each of the three subdomains, it is often useful to construct composite solutions that are uniformly valid throughout the entire domain. For a system possessing a leading-order outer expansion given by $h_0^{\text{out}}(x)$ and a leading-order inner expansion given by $h_0^{\text{in}}(s)$, where x is the outer independent variable and s is the inner independent variable, the leading-order composite expansion h_0^{comp} is given by

$$h_0^{\text{comp}} = h_0^{\text{out}} + h_0^{\text{in}} - h_0^{\text{match}}. \quad (3.106)$$

Here the outer and the inner expansions must be expressed in the same independent variable, and h_0^{match} is given by

$$h_0^{\text{match}} = \lim_{s\to\infty} h_0^{\text{in}}(s) = \lim_{x\to 0} h_0^{\text{out}}(x). \quad (3.107)$$

The leading-order electron and ion densities on the geometric length scale are of order one. Relative to this density the leading-order electron and ion density on the mean-free-path scale is of order δ_i. Similarly, the leading-order contributions to the electron and ion densities on the sheath scale were found to be of order $\delta_d^{\overline{\nu}} = \delta_i$. So the only contribution to the leading-order composite solution for the electron and ion density comes from the solution on the geometric length scale. Upon writing this solution in terms of the sheath variable given by

$$\theta = \delta_d^{\overline{\nu}}\xi + 1, \quad (3.108)$$

the composite solutions for the ion density η_{i00}^c and for the electron density η_{e00}^c are expressed as

$$\eta_{i00}^c = \eta_{e00}^c = \text{sn}\left(-\frac{\delta_n}{k\delta_r}\delta_d^{\overline{\nu}}\theta, k\right). \quad (3.109)$$

The leading-order contribution to the ion and electron velocities on the geometric scale is of order δ_i. The leading-order contribution to these velocities on the mean-free-path scale is of order one. On the sheath scale, the electron and ion velocities are also of order one. Therefore the contributions to the leading-order composite expansion for the electron and ion velocities comes from the mean-free-path and the sheath scale solutions. These composite expansions may be written as

$$u_{i00}^c = \overline{u}_{i00} + \widetilde{u}_{i00} - \lim_{\zeta\to 0^-}\overline{u}_{i00}, \quad (3.110)$$

$$u_{e00}^c = \overline{u}_{e00} + \widetilde{u}_{e00} - \lim_{\zeta\to 0^-}\overline{u}_{e00}. \quad (3.111)$$

Upon substituting the appropriate solutions and writing them in the sheath

https://doi.org/10.1017/S0022377898006497 Published online by Cambridge University Press

coordinate, these composite expansions become

$$u^c_{i00} = \frac{1}{2}\left(\frac{\delta_T^{1/2} + \frac{1}{2}\delta_m^{1/2}}{1+\delta_m}\frac{\delta_d^{\overline{\nu}}}{\delta_i}\theta - 2\frac{1+\delta_T}{1+\delta_m}\right) \times \left\{-1 + \left[1 - \frac{4\dfrac{1+\delta_T}{1+\delta_m}}{\left(\dfrac{\delta_T^{1/2} + \frac{1}{2}\delta_m^{1/2}}{1+\delta_m}\dfrac{\delta_d^{\overline{\nu}}}{\delta_i}\theta - 2\dfrac{1+\delta_T}{1+\delta_m}\right)^2}\right]^{1/2}\right\} + \widetilde{u}_{i00}(\theta) - \left(\frac{1+\delta_T}{1+\delta_m}\right)^{1/2}, \tag{3.112}$$

$$u^c_{e00} = \frac{1}{2}\left(\frac{\delta_T^{1/2} + \frac{1}{2}\delta_m^{1/2}}{1+\delta_m}\frac{\delta_d^{\overline{\nu}}}{\delta_i}\theta - 2\frac{1+\delta_T}{1+\delta_m}\right) \times \left\{-1 + \left[1 - \frac{4\dfrac{1+\delta_T}{1+\delta_m}}{\left(\dfrac{\delta_T^{1/2} + \frac{1}{2}\delta_m^{1/2}}{1+\delta_m}\dfrac{\delta_d^{\overline{\nu}}}{\delta_i}\theta - 2\dfrac{1+\delta_T}{1+\delta_m}\right)^2}\right]^{1/2}\right\} + \widetilde{u}_{e00}(\theta) - \left(\frac{1+\delta_T}{1+\delta_m}\right)^{1/2}, \tag{3.113}$$

where $\widetilde{u}_{i00}$ and $\widetilde{u}_{e00}$ are determined by numerical integration of (3.98) and (3.100).

Finally, the leading-order composite solution for the potential is constructed. Leading-order contributions to this solution come from all three subdomains. This composite solution is given by

$$\phi^c_{00} = \phi_{00} + \overline{\phi}_{00} + \widetilde{\phi}_{00} - \lim_{\xi\to 1}\phi_{00} - \lim_{\zeta\to 0^-}\overline{\phi}_{00}. \tag{3.114}$$

Written in terms of the sheath independent variable, this solution becomes

$$\phi^c_{00} = \frac{\delta_T^{1/2} - \frac{1}{2}\delta_m^{1/2}\delta_T}{\delta_T^{1/2} + \frac{1}{2}\delta_m^{1/2}}\ln\left[-\frac{\delta_r k}{\delta_n}\frac{1}{\delta_d^{\overline{\nu}}\theta}\mathrm{sn}\left(-\frac{\delta_n}{k\delta_r}\delta_d^{\overline{\nu}}\theta, k\right)\right] + \frac{\delta_T^{1/2} - \frac{1}{2}\delta_m^{1/2}\delta_T}{\delta_T^{1/2} + \frac{1}{2}\delta_m^{1/2}}\ln\left(\delta_i\overline{\eta}_{i00}\frac{\delta_d^{\overline{\nu}}}{\delta_i}\theta\right) - \frac{1}{2}\frac{\frac{1}{2}\delta_m^{1/2} - \delta_m\delta_T^{1/2}}{\delta_T^{1/2} + \frac{1}{2}\delta_m^{1/2}}\overline{u}^2_{i00}\frac{\delta_d^{\overline{\nu}}}{\delta_i}\theta - \frac{1}{2}(\widetilde{u}^2_{i00} - \delta_T\ln\widetilde{u}^2_{i00}) + \frac{1}{2}\frac{1+\delta_T}{1+\delta_m} - \frac{1}{2}\delta_T\ln\left(\frac{1+\delta_T}{1+\delta_m}\right). \tag{3.115}$$

The composite solutions given here are uniformly valid to leading order in the parameters δ_i and δ_d in the entire domain $0 \leqslant \xi \leqslant 1$.

https://doi.org/10.1017/S0022377898006497 Published online by Cambridge University Press

Table 1. Leading-order physical phenomena.

Scale	Inertia	Pressure	Field	Collisions	Sources	Charge
Geometric		✓	✓	✓	✓	
MFP	✓	✓	✓	✓		
Sheath	✓	✓	✓			✓

4. Discussion

In this paper, approximate solutions to the equations describing the region of a dense, low-temperature plasma adjacent to a non-emitting wall have been obtained using the method of matched asymptotic expansions. At leading order, the boundary region has been found to consist of three overlapping layers with different physical phenomena dominating the model in each layer. The dominant physical phenomena in each layer is summarized in Table 1. On the geometric length scale, which extends to the symmetry boundary, the plasma is quasineutral, and the motion of the electrons and ions is primarily governed by ambipolar diffusion. This region is marked by the departure of the electron and ion densities from ionization equilibrium. Ionization equilibrium is approached, in an asymptotic sense, as the number of recombination lengths from the wall is increased. The ion velocity in this region is very small, and is therefore rescaled such that the reference velocity scale becomes the velocity derived from mobility-limited flow.

On the mean-free-path scale, ion inertia, which was negligible on the geometric length scale, becomes a leading-order influence. A consequence of including this leading-order phenomenon is that the velocities and densities are rescaled in this region. The velocity is scaled down, returned to its original scale, since the ions are accelerated from a very small value to the sonic velocity. The density is scaled up since the mean free path layer is very near the wall where the charged particle density becomes very small. The ion and electron source terms in the continuity equations are not of leading order on this scale owing to the small densities. The ion motion in this layer is analogous to the one-dimensional flow of a compressible fluid, without friction, mass addition or heat addition, in that it cannot be accelerated beyond the sound speed. In order to accelerate the ions further, the influence of space charge must be included.

Immediately adjacent to the wall is the sheath, on the Debye scale, in which the influence of space charge becomes important. In the sheath, the particle source terms are not of leading order, and the collision terms become of less than leading order. The principal leading-order influence in the sheath, the space-charge influence, is governed by the Poisson equation which first becomes of leading order on this scale. Defining the sheath boundary to be the point at which the ions become sonic, satisfying the equality in Bohm's criterion, is only valid at leading order in the Debye length. At higher order, the influence of space charge appears in the presheath.

4.1. Comparisons with existing solutions

The solutions obtained for the symmetric problem on the geometric length scale, upon transformation to the semi-infinite geometry, can be shown to agree with the solutions obtained by Self and Eskin (1983). In order to illustrate this agreement, the equilibrium density is made the reference density, by setting $\delta_n = 1$, which makes the modulus k of the Jacobi elliptic functions equal to 1. Upon making the

https://doi.org/10.1017/S0022377898006497 Published online by Cambridge University Press

recombination length the reference length, by setting $\delta_r = 1$, and translating the origin to the wall, by letting $\xi^* = 1 - \xi$, which reverses the coordinate direction, the argument of the elliptic functions simply becomes $u = \xi^*$. When the modulus of the Jacobi elliptic functions is 1, these functions reduce to the hyperbolic functions such that $\mathrm{sn}(u, 1) = \tanh u$ and $\mathrm{cn}(u, 1) = \mathrm{dn}(u, 1) = \mathrm{sech}\, u$. Upon making these transformations to the solutions on the geometric length scale, the results

$$\eta_{i00} = \eta_{e00} = \tanh\ \xi^*, \tag{4.1}$$

$$u_{is00} = u_{es00} = \frac{-2}{1 + \frac{1}{2}\delta_m^{1/2}} \mathrm{sech}^2\, \xi^* \coth\, \xi^*, \tag{4.2}$$

$$\phi_{00} = \frac{1 - \frac{1}{2}\delta_m^{1/2}}{1 + \frac{1}{2}\delta_m^{1/2}} \ln(\tanh \xi^*) \tag{4.3}$$

are obtained. These solutions are identical to those obtained for the quasineutral model in a semi-infinite geometry analysed by Self and Eskin (1983) in the limit of zero net current.

In order to compare the solutions obtained in this work with other existing solutions, it is useful to approximate the electron and ion sources by a linear source model. Most existing solutions for the presheath that account for particle sources take the rate of production of electron–ion pairs to be proportional to the electron density, with the constant of proportionality being a net ionization frequency. Solutions using a linear source can be approximated by modifying the electron and ion sources in the continuity equations. The electron and ion sources are modified as

$$S_{i,e} = 2a_s^2 \delta_i \frac{\delta_n^2}{\delta_r^2} \frac{1 + \delta_T}{\delta_T^{1/2} + \frac{1}{2}\delta_m^{1/2}} \eta_e \left(\frac{1}{\delta_n^2} - b_s^2 \eta_i \eta_e \right), \tag{4.4}$$

where, for the nonlinear source $a_s^2 = b_s^2 = 1$, and for the linear source $b_s^2 = 0$ and

$$a_s^2 = \nu_s \frac{\delta_r^2}{2\delta_i} \frac{\delta_T^{1/2} + \frac{1}{2}\delta_m^{1/2}}{1 + \delta_T}. \tag{4.5}$$

Here ν_s is the ionization frequency ν_I normalized by $(k_b T_e/m_i)^{1/2}/L$.

By using this modified source, and following through with the solutions as before, the argument of the Jacobi elliptic functions becomes

$$u = K(k) - a_s \frac{b_s \delta_n}{\delta_r k} \xi, \tag{4.6}$$

where the modulus has been redefined as

$$k = \left(\frac{b_s^2 \delta_n^2}{2 - b_s^2 \delta_n^2} \right)^{1/2}. \tag{4.7}$$

The condition for matching the outer density with the density on the mean-free-path scale leads to the requirement that

$$a_s \frac{b_s \delta_n}{\delta_r k} = K(k). \tag{4.8}$$

For the linear source $b_s = 0$, and the modulus of the elliptic functions is zero. When the modulus is zero, the Jacobi elliptic functions reduce to circular functions,

https://doi.org/10.1017/S0022377898006497 Published online by Cambridge University Press

such that $\mathrm{sn}(u,0) = \sin u$, $\mathrm{cn}(u,0) = \cos u$, and $\mathrm{dn}(u,0) = 1$, and the complete elliptic integral becomes $K(0) = \frac{1}{2}\pi$. This renders the condition above as

$$a_s \frac{\sqrt{2}}{\delta_r} = \frac{\pi}{2}, \tag{4.9}$$

or

$$\nu_I = \delta_i \frac{\pi^2}{4} \frac{1+\delta_T}{\delta_T^{1/2} + \frac{1}{2}\delta_m^{1/2}} \frac{(k_b T_e/m_i)^{1/2}}{L}, \tag{4.10}$$

which is the familiar result that the ionization frequency cannot be independent of both plasma conditions (species, electron temperature and ion temperature) and the distance to the wall. This condition ensures that the rate at which ions and electrons are generated in the volume of the discharge must be balanced by the rate at which they are absorbed at the wall. So, for the linear ionization source, the leading-order solutions on the geometric length scale become

$$\eta_{i00} = \eta_{e00} = \sin[\tfrac{1}{2}\pi(1-\xi)] = \cos(\tfrac{1}{2}\pi\xi), \tag{4.11}$$

$$u_{is00} = u_{es00} = \frac{\pi}{2} \frac{1+\delta_T}{\delta_T^{1/2} + \frac{1}{2}\delta_m^{1/2}} \tan(\tfrac{1}{2}\pi\xi), \tag{4.12}$$

$$\phi_{00} = \frac{\delta_T^{1/2} - \frac{1}{2}\delta_m^{1/2}}{\delta_T^{1/2} + \frac{1}{2}\delta_m^{1/2}} \ln[\cos(\tfrac{1}{2}\pi\xi)]. \tag{4.13}$$

These are the well-known solutions from linear, ambipolar diffusion theory.

By using these solutions for the linear source approximation, composite solutions for the presheath region can be constructed from the solutions on the geometric and mean-free-path length scales. These composite solutions may then be compared with the presheath solutions developed by Self and Ewald (1966). Self and Ewald were able to obtain an analytical solution valid in the entire presheath region because they made the linear source approximation and they neglected electron inertia.

The composite presheath solutions for the electron and ion densities are simply the geometric-scale solutions, since the density scales as δ_i in the mean free path layer. Also, the composite presheath solutions for the electron and ion velocities are given by the mean-free-path-scale solutions, since the velocity scales as δ_i on the geometric length scale. The composite solution for the potential in the presheath must be constructed from contributions on both the geometric and mean-free-path length scales, and is determined to be

$$\phi_{00}^c\Big|_{\substack{\text{linear}\\ \text{source}}} = \frac{\delta_T^{1/2} - \frac{1}{2}\delta_m^{1/2}\delta_T}{\delta_T^{1/2} + \frac{1}{2}\delta_m^{1/2}} \left\{ \ln\left[\frac{\cos\left(\frac{1}{2}\pi\xi\right)}{\frac{1}{2}\pi\left(1-\xi\right)}\right] + \ln\left(\delta_i \frac{\pi}{2} \frac{1+\delta_T}{\delta_T^{1/2} + \frac{1}{2}\delta_m^{1/2}} \frac{1}{\overline{u}_{i00}}\right)\right\}$$
$$- \tfrac{1}{4}\delta_m^{1/2} \frac{1 - 2\delta_m^{1/2}\delta_T^{1/2}}{\delta_T^{1/2} + \frac{1}{2}\delta_m^{1/2}} \overline{u}_{i00}^2. \tag{4.14}$$

Self and Ewald (1966) expressed their solutions in terms of two parameters R' and

https://doi.org/10.1017/S0022377898006497 Published online by Cambridge University Press

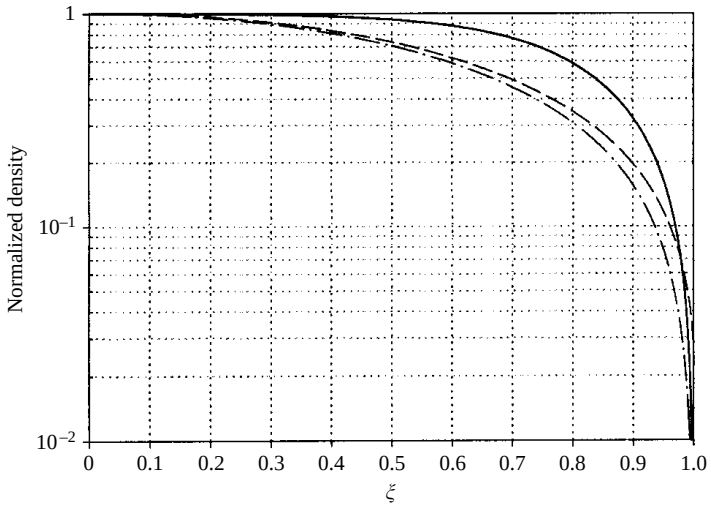


Figure 1. Presheath density profiles for linear (—·—·) and nonlinear (——) electron and ion sources, together with the Self and Ewald solution (– –) (Ar, mean free path/geometric length = 0.01).

A, which can be expressed in terms of the nomenclature used here as

$$R' = \frac{\delta_i \nu_s + \delta_T^{1/2}}{\delta_i \delta_m \nu_s + \frac{1}{2}\delta_m^{1/2}}, \qquad A = \frac{\delta_i \nu_s}{\delta_i \nu_s + \delta_T^{1/2}}. \tag{4.15}$$

In Fig. 1 the solution for the electron and ion densities in the presheath region is shown, for an argon plasma with $\delta_i = 0.01$, for both linear and nonlinear source terms. The composite presheath solution with the linear source term agrees with the analytical solution of Self and Ewald (1966) to within a difference of order δ_i. This agreement is as good as can be expected for the leading-order composite solution, since the first-order correction to the density, which is of order δ_i, has been neglected. The neglect of the first-order influence is most prominent very near the wall, which is to be expected since the lowest-order contribution to the density on the mean-free-path scale is of order δ_i, and therefore is not part of the composite solution presented here.

Also shown in this figure is the composite solution for the density profile in the presheath using the nonlinear electron and ion source. Here it is observed that accounting for ionization nonequilibrium, by including three-body recombination influences, produces a broadening of the density profile, with the pronounced decrease in density, as the wall is approached, occurring closer to the wall. In other words, the plasma remains nearly in ionization equilibrium for a greater fraction of the distance from the plane of symmetry to the wall. This result is consistent with the trend shown, and briefly discussed, by Franklin (1976) for the case of linear, ambipolar diffusion in the cylindrical positive column. Franklin showed the same broadening of the density profile for an increasing recombination coefficient.

The presheath solution for the electron and ion velocity for this case is shown in Fig. 2. Here the best agreement between the composite solution and the analytical solution of Self and Ewald (1966) is near the wall. This agreement is as expected, since the leading-order composite solution for the velocity is constructed entirely

https://doi.org/10.1017/S0022377898006497 Published online by Cambridge University Press

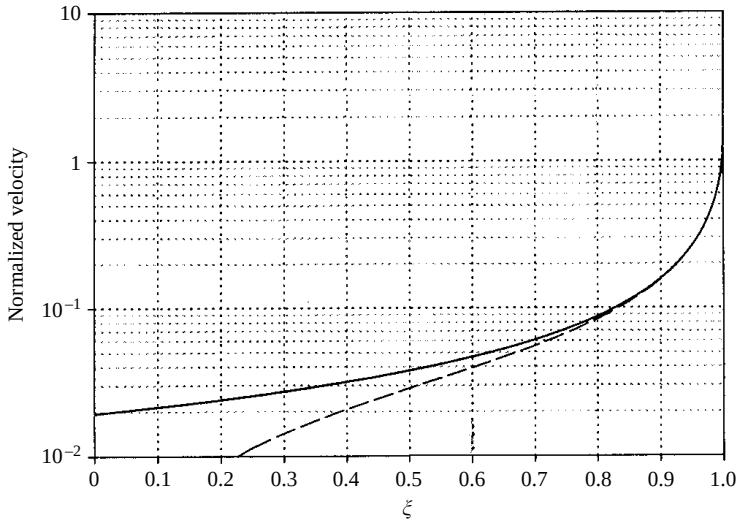


Figure 2. Presheath velocity profiles for linear and nonlinear electron and ion sources (——), together with the Self and Ewald solution (– –) (Ar, mean free path/geometric length = 0.01).

from the leading-order solution on the mean-free-path scale, which is most accurate near the wall. Away from the wall, the composite solution agrees with the solution of Self and Ewald (1966) to within a difference of order δ_i (the Self and Ewald solution is zero at $\xi = 0$). This agreement is consistent with the fact that the lowest-order contribution to the velocity on the geometric scale is of order δ_i, and is therefore neglected in the leading-order composite solution. The solution for the velocity on the mean-free-path scale is the same whether the linear or nonlinear source is assumed, since the source terms are not of leading order on this scale.

The solutions for the presheath potential are shown in Fig. 3. The composite presheath solution is shown to agree exceptionally well with the solution reported by Self and Ewald (1966). Recall that the composite solution for the potential is constructed from contributions on both the geometric and the mean-free-path scales, which results in this relatively uniform agreement. When the nonlinear electron and ion sources are used, the potential profile exhibits the broadening noted in the density profile. The region in which the potential increases to its value at the sheath edge, the presheath potential, is compressed closer to the sheath edge. Also, for the conditions here, the absolute value of the normalized presheath potential is increased by 27%, from 3.0 to 3.8, when the linear source approximation is made. In general, this difference in the presheath potential could be greater or less than zero depending on the particular plasma conditions. In these particular conditions, the larger gradient in density, as the wall is approached, indicates that diffusion plays a more significant role in accelerating the ions for the nonlinear source than it does for the linear source. Therefore the potential difference does not have to be as large in order to accelerate the ions to the Bohm speed.

The difference in presheath potential, $\Delta\phi_{ps}$, can be generalized by subtracting the composite solution for the potential with the linear source term from the solution

https://doi.org/10.1017/S0022377898006497 Published online by Cambridge University Press

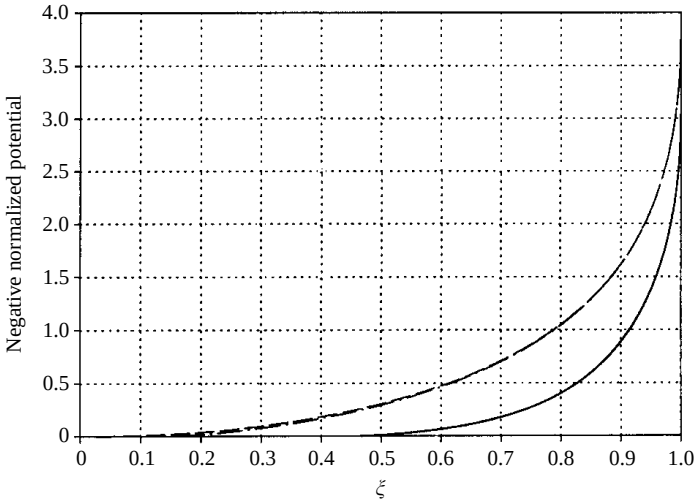


Figure 3. Presheath potential profiles for linear (–·–·) and nonlinear (——) electron and ion sources, together with the Self and Ewald solution (– –) (Ar, mean free path/geometric length = 0.01).

with the nonlinear source term to obtain

$$\Delta\phi_{ps} = \frac{\delta_T^{1/2} - \frac{1}{2}\delta_m^{1/2}\delta_T}{\delta_T^{1/2} + \frac{1}{2}\delta_m^{1/2}} \ln\left(\frac{2}{\pi}\frac{\delta_n}{\delta_r k}\right). \tag{4.16}$$

As the recombination length becomes smaller the influence of electron–ion recombination influences the presheath potential profile more significantly.

On the sheath scale, the electron and ion sources are not of leading–order; therefore the leading-order governing equations in the sheath are identical to those obtained by Friedman (1967) for his linear source model, despite the fact that Friedman did not account for a completely general scaling. Since the sheath equations in this model are identical to Friedman's, the solutions to the sheath solutions are also identical although the scales are different. The two models differ in the asymptotic matching conditions. The influence of the nonlinear source on the sheath solutions is introduced through the asymptotic matching to the presheath solution.

4.2. Solution evaluations

In order to facilitate a discussion of the results from this analysis, a representative thermal plasma, taken to be argon at 100 Torr, with $T_e = T_i = 15\,000\,\mathrm{K}$ (1.3 eV) and with a channel width of 6 cm is considered. Under these conditions, $\delta_r = 0.12$, $\delta_i = 8.6 \times 10^{-4}$ and $\delta_d = 4.4 \times 10^{-6}$.

The solutions for density, velocity, and potential on the geometric length scale for these representative conditions are illustrated in Fig. 4. In this figure the characteristic decrease in density as the wall is approached is apparent. For these particular conditions, $\delta_n \approx 1.0$, which means that the electron and ion densities on the centreline are practically in ionization equilibrium. With δ_n this close to 1.0, the solution for the density very nearly has the behaviour of the hyperbolic tangent. Also in Fig. 4, it is apparent that the scale on which the velocity tends to infinity, is longer than the scale on which the potential tends to infinity, indicating the relative magnitudes of the mean-free-path layer and the sheath.

https://doi.org/10.1017/S0022377898006497 Published online by Cambridge University Press

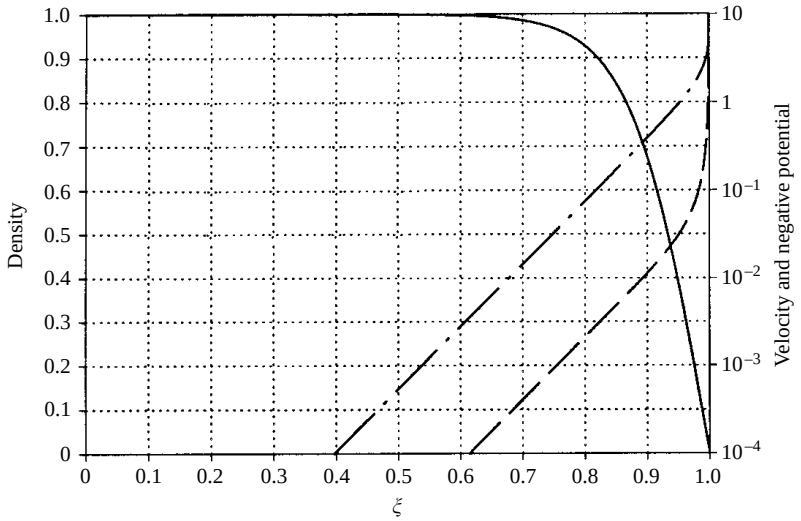


Figure 4. Solutions on the geometric length scale for Ar at 100 Torr with $T_e = T_i = 15\,000$ K: ——, density; – –, velocity, - — -, potential.

The electron and ion velocities scale differently on the geometric and mean-free-path scales. Recall that on the geometric scale, the lowest-order contribution to the velocity is of order δ_i while on the mean free path scale, the lowest-order contribution is of order 1. The solutions for the velocity on the geometric and mean-free-path scales are shown in Fig. 5. In this figure, the removal of the singularity at the wall in the geometric-scale solution by the correction introduced on the mean-free-path scale is observed. The normalized velocity at the wall on the mean-free-path scale is $[(1 + \delta_T) / (1 + \delta_m)]^{1/2}$, which for these conditions is approximately equal to 1.4.

The solutions for the potential on both the geometric and mean-free-path scales are also shown in Fig. 5. As with the velocity, the singularity in the geometric-scale solution is removed by the correction to the potential on the mean-free-path scale. The value of the potential at the wall in the mean-free-path solution is approximately -4.6. Since the potential is normalized by the electron temperature, this means that the voltage drop from the plane of symmetry to the 'edge' of the mean-free-path region, the presheath voltage, is about -6 V. This is the voltage required to accelerate the ions, created at rest, to the velocity that satisfies the two-temperature version of Bohm's criterion. The value of the presheath voltage for these conditions, a highly collisional plasma, is considerably larger than it is for collisionless plasmas, where the acceleration of ions is impeded only by their inertia. For collisionless plasmas, presheath voltages are typically of the order of 1 times $k_b T_e/e$. Note that while the potential is not singular at the sheath edge, $\zeta = 0$, the electric field is singular. This field singularity indicates the transition to the sheath.

The sheath region was determined to scale as $\delta_d^{(1-0.5 \ln \delta_i / \ln \delta_d)}$ such that

$$\theta = (1 - \xi) / \delta_d^{(1-0.5 \ln \delta_i / \ln \delta_d)}. \tag{4.17}$$

The electron and ion densities on the sheath scale were determined to scale equivalent to the density on the mean-free-path scale. The solutions for the electron and

https://doi.org/10.1017/S0022377898006497 Published online by Cambridge University Press

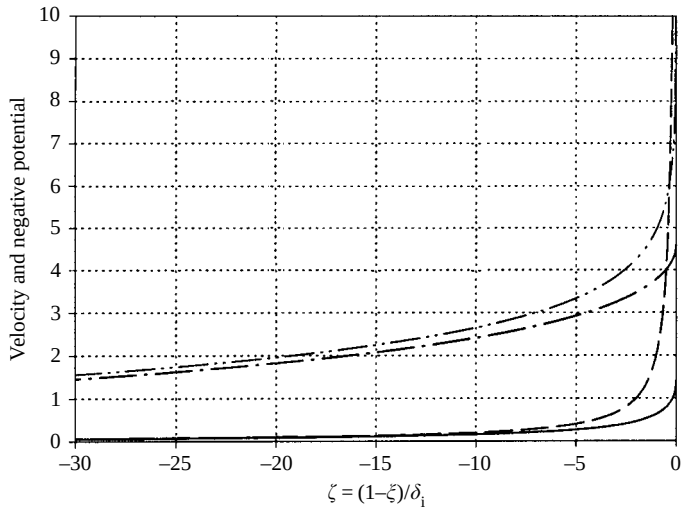


Figure 5. Velocity (——) and potential (-·—·-) on the mean-free-path scale, and velocity (– –) and potential (- - ·—· - -) on the geometric scale for Ar at 100 Torr and $T_e = T_i = 15\,000$ K.

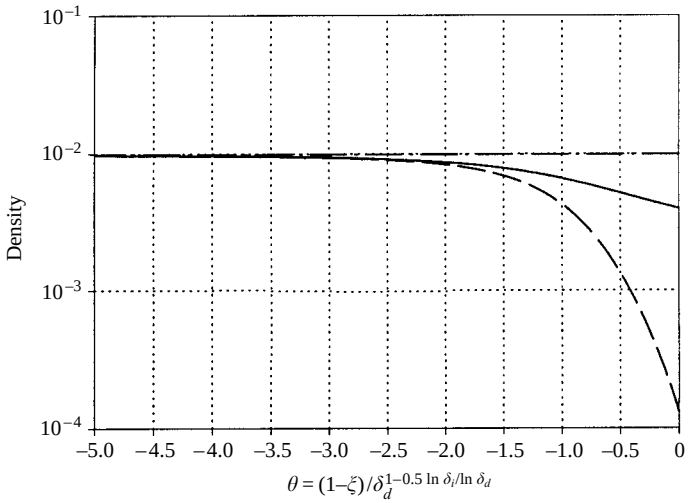


Figure 6. Electron (– –) and ion (——) densities on the Debye length scale for Ar at 100 Torr with $T_e = T_i = 15\,000$ K, together with the densities on the mean-free-path scale (-·—·- for both electrons and ions).

ion densities in the sheath are shown in Fig. 6. Also shown in this figure is the solution for the density at $\zeta = 0$ on the mean-free-path scale. In this figure, the separation of the electron and ion densities, which produces the space charge characterizing the sheath, is clear. It is this space charge that produces the potential drop in the sheath. The approach of the solution for the density in the sheath to the presheath solution at $\zeta = 0$ is apparent in this figure. The extent of the space charge characterizing the sheath appears to be about 3–5 units of the sheath coordinate.

The electron and ion velocities on the sheath scale are shown in Fig. 7. The velocity in the sheath scales equivalently to the velocity on the mean-free-path length

https://doi.org/10.1017/S0022377898006497 Published online by Cambridge University Press

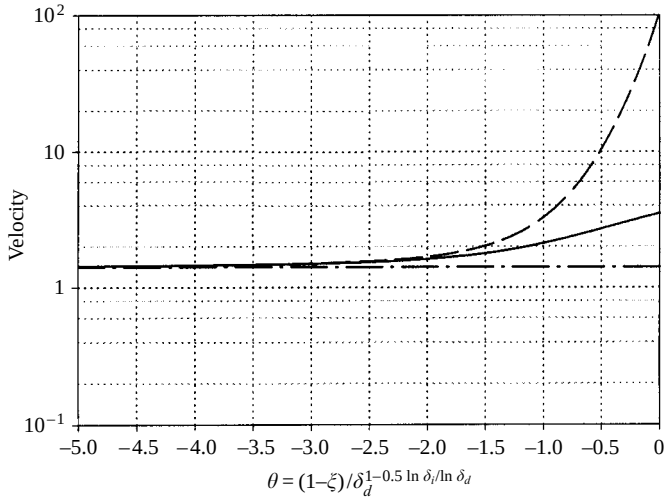


Figure 7. Electron (– –) and ion (—) velocities on the Debye length scale for Ar at 100 Torr and $T_e = T_i = 15\,000$ K, together with the velocities on the mean-free-path scale (- — - for both electrons and ions).

scale. The ion velocity at the wall is approximately 6.2 km s^{-1}, which corresponds to a kinetic energy of 1.3×10^{-18} J per impacting ion. The electron velocity at the wall is approximately 19 km s^{-1}, since only the electrons in the high-energy tail of the Maxwellian velocity distribution can overcome the potential barrier and make it to the wall. As $\theta \to -\infty$ the electron and ion velocities approach the same value which, as Fig. 7 illustrates, is equivalent to the value of the velocity on the mean-free-path scale at $\zeta = 0$.

The solution for the electric potential on the sheath scale is shown in Fig. 8. The potential at the wall is approximately −11.5 V, and, as $\theta \to -\infty$, the potential asymptotes to the value at the edge of the presheath ($\zeta = 0$ on the mean-free-path scale), which was noted earlier as −6 V. This makes the voltage drop across the sheath −5.5 V, whereas the simple estimate for the sheath voltage, $-(k_b T_e/e)\ln[(2\pi\delta_m)^{-1/2}]$, is −6.1 V. The correction to the sheath voltage, which results from the asymptotic matching to the presheath solutions, for this case is therefore about 10 %.

Finally, the composite solutions are evaluated. The leading-order composite solutions for the plasma conditions considered here are illustrated in Fig. 9. Since the mean-free-path and sheath scales are so small, the influence of these layers can hardly be seen on the scale of this plot. The region near the wall is expanded in Fig. 10. In this figure the separation of the ion and electron velocities, and the potential increase to its value at the wall are apparent.

In order to explore further the influence of the nonlinear source on the solution for the wall potential, (3.103) is examined closely. It is interesting to note that the first term on the right-hand side of this equation is the value of the sheath potential obtained from simple sheath theory, based on cold, collisionless ions and Boltzmann-distributed electrons, in which the presheath potential is defined to be zero. The additional terms on the right-hand side of this expression represent a correction to the wall potential, which results from matching the sheath solution with the presheath. The difference between the wall potential for the case with

https://doi.org/10.1017/S0022377898006497 Published online by Cambridge University Press

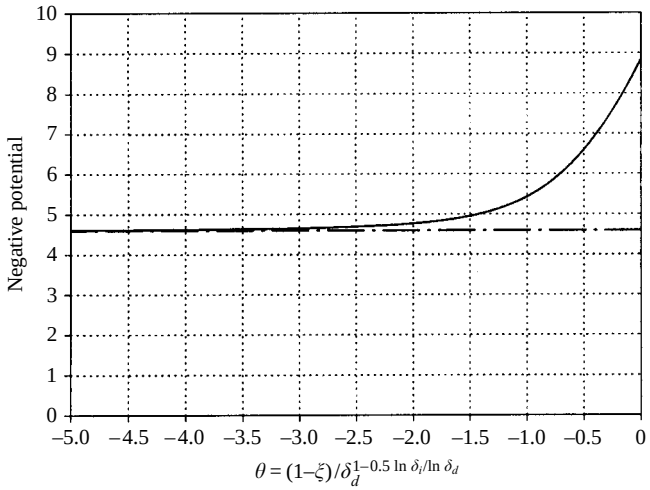


Figure 8. Potentials on the Debye (——) and mean-free-path (- — -) length scales for Ar at 100 Torr and $T_e = T_i = 15\,000$ K.

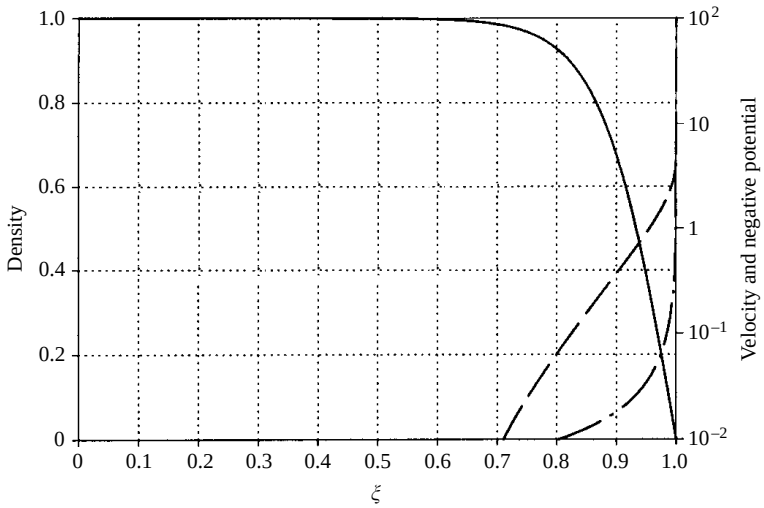


Figure 9. Composite solutions for Ar at 100 Torr and $T_e = T_i = 15\,000$ K: ——-, density; - — -, electron and ion velocity; – –, potential.

the nonlinear source and that for the case with the linear source is identical to the difference in the presheath solution, given by (4.16). Therefore the shape of the potential profile is not altered by assuming a linear or nonlinear source – it is merely shifted in magnitude by the matching condition. This is a consequence of the fact that there is no influence from the source term in the potential difference across the sheath given in (3.105).

The ion velocity at the wall, derived from (3.102), is not altered by choosing a linear or nonlinear source. This is a consequence of the fact that the ions enter the sheath at the Bohm speed and are accelerated to the wall by mechanisms that are independent of the electron and ion sources. The primary accelerating force is the field that results from charge separation. However, the ion flux to the wall can be

https://doi.org/10.1017/S0022377898006497 Published online by Cambridge University Press

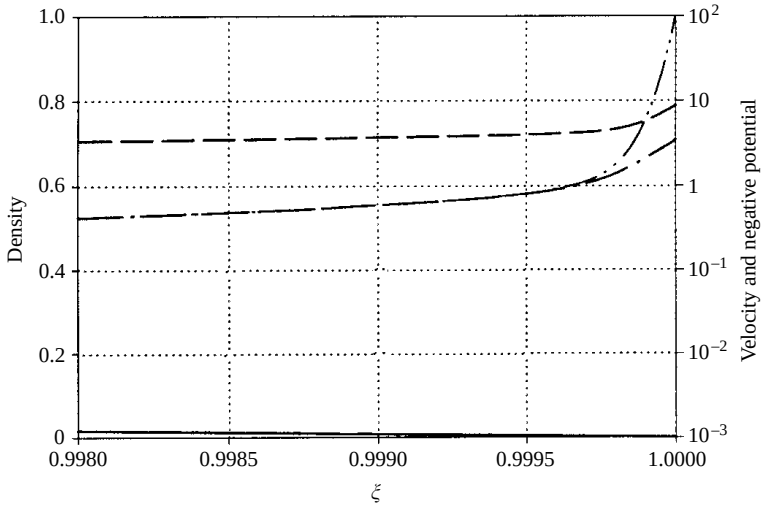


Figure 10. Composite solutions, magnified near the wall, for Ar at 100 Torr and $T_e = T_i =$ 15 000 K: ——, density; -—-, ion velocity; - - —- -, electron velocity; ––, potential.

significantly affected by the type of source. The power flux to the wall, resulting from the kinetic energy imparted by impacting ions, is obtained by multiplying the ion kinetic energy at the wall and the ion flux at the wall. Upon subtracting the expression for this power flux, derived from solutions with the nonlinear source, from the power-flux expression derived from solutions with the linear source, the difference

$$\Delta P_k = \frac{1}{2}u_w^2 \frac{1+\delta_T}{\delta_T^{1/2} + \frac{1}{2}\delta_m^{1/2}} n_{eq} \frac{k_b T_e^{3/2}}{m_i^{1/2}} \left(\frac{\delta_n}{\delta_r k} - \frac{\pi}{2} \right) \tag{4.18}$$

is obtained. For conditions in which recombination is important, δ_n and k are typically closer to 1, and δ_r is small. Therefore the computed power flux to the wall is strongly influenced by the source model. Of course, this 'kinetic' power flux may only be a fraction of the total power flux to the wall when local and nonlocal heat conduction, as well as radiation, are considered.

5. Concluding remarks

In summary, asymptotically matched solutions for electron and ion densities electron and ion velocities, and electric potential have been obtained on the geometric, mean-free-path and Debye length scales for the case of a dense, low-temperature plasma adjacent to a perfectly absorbing wall. The leading-order, geometric-scale solutions have been obtained in terms of the Jacobi elliptic functions. These solutions have been shown to reduce to hyperbolic functions in the case of a semi-infinite geometry and to circular functions for the case of linear-source, ambipolar diffusion.

The scale of the sheath was determined to be $\delta_d^{1-0.5\ln\delta_i/\ln\delta_d}$. In a previous analysis of the plasma boundary region, presented by Friedman (1967), the possibility that the density would need to be scaled in the sheath region was briefly discussed, but in that work consideration was limited to the low-pressure regime and the density scaling was neglected. A consequence of the scaling that leads to the sheath scale

https://doi.org/10.1017/S0022377898006497 Published online by Cambridge University Press

is that in order for the scale of the sheath to be much less than the scale of the mean-free-path layer, it must hold that $\delta_d^{\overline{\nu}} \ll \delta_i$. By using the expression derived in Sec. 3 that relates $\overline{\nu}$ to δ_d and δ_i, this condition reduces to $\delta_d^{2/3} \ll \delta_i$.

Leading-order composite solutions valid throughout the boundary region have been constructed from the leading-order solutions in each of these subdomains. These composite solutions have been used to assess the impact of accounting for electron–ion recombination in the ionization nonequilibrium region on sheath and presheath profiles, and on quantities evaluated at the wall. While, at leading order, the velocity profiles throughout the boundary region are not influenced by recombination, the density and potential profiles do show pronounced differences when recombination is included.

When recombination is included, both the density and potential profiles show significant broadening. This broadening results in the region of rapid change in these profiles being compressed closer to the wall. The difference in the presheath potential that results from accounting for recombination has been determined to scale as $\ln[(2/\pi)\delta_n/\delta_r k]$. This difference shifts the sheath potential profile, resulting in a different value of the wall potential. The spreading of the density profile results in a larger flux of ions accelerating through the sheath and impacting on the wall. The difference in the ion power flux to the wall resulting from recombination has been determined to scale as $\delta_n/\delta_r k - \frac{1}{2}\pi$.

Acknowledgements

The authors gratefully acknowledge useful and informative discussions with Professor Marc K. Smith and Dr Jad H. Batteh.

References

Bohm, D. 1949 *The Characteristics of Electrical Discharges in Magnetic Fields* (ed. A. Guthry and R. K. Wakerling). McGraw-Hill, New York.

Franklin, R. N. 1976 *Plasma Phenomena in Gas Discharges*, Chap. 5. Oxford University Press.

Franklin, R. N. and Ockendon, J. R. 1970 *J. Plasma Phys.* **4**, 371.

Friedman, H. W. 1967 *Phys. Fluids* **10**, 2053.

Persson, K.-B. 1962 *Phys. Fluids* **5**, 1625.

Riemann, K.-U. 1991 *J. Phys. D: Appl. Phys.* **24**, 493.

Self, S. A. and Eskin, L. D. 1983 *IEEE Trans. Plasma Sci.* **11**, 279.

Self, S. A. and Ewald, H. N. 1966 *Phys. Fluids* **9**, 2486.

Thornhill, L. D. 1996 Boundary layers in dense, low-temperature plasmas. PhD dissertation, Georgia Institute of Technology.

Tonks, L. and Langmuir, I. 1929 *Phys. Rev.* **34**,876.

Zel'dovich, Ya. B. and Raizer, Yu. P. 1966 *Physics of Shock Waves and High-Temperature Hydrodynamic Phenomena*, Vol. 1. Academic Press, New York.

https://doi.org/10.1017/S0022377898006497 Published online by Cambridge University Press